

An analysis of limit cycles in glacier-dammed lake systems: Supplementary material

Christian Schoof

Department of Earth, Ocean and Atmospheric Sciences,
University of British Columbia,
2207 Main Mall, Vancouver, Canada, V6T 1Z4
`cschoof@eos.ubc.ca`

June 2, 2019

1 An introductory note

The purpose of these notes is to provide mathematical detail for the results presented in the main paper. To make these notes more continuously readable, some of the material in the main paper (specifically the linear stability analysis) is repeated below.

2 Model

2.1 A spatially extended model

The main paper uses two closely related models to study the dynamics of glacier-dammed lake systems. The first is the spatially one-dimensional model of Schoof and others (2014) described in this subsection, while the second is a lumped version detailed in section 2.3. The former is a slightly simplified version of the more general form

$$\frac{\partial S}{\partial t} = c_1 q \Psi + v_o(S) - v_c(S, N) \quad (1a)$$

$$\frac{\partial S}{\partial t} + \frac{\partial q}{\partial x} = r c_1 q \Psi \quad (1b)$$

$$q = q(S, \Psi) \quad (1c)$$

$$\Psi = \Psi_0 + \frac{\partial N}{\partial x} \quad (1d)$$

on $0 < x < L$, subject to boundary conditions

$$-V_p(N) \frac{\partial N}{\partial t} = q_{in} - q \quad \text{at } x = 0 \quad (1e)$$

$$N = 0 \quad \text{at } x = L \quad (1f)$$

Here, $S(x, t) > 0$ is conduit cross-section, $N(x, t)$ is effective pressure, $\Psi(x, t)$ is hydraulic gradient, $q(S, \Psi)$ is discharge through the conduit, t is time and x is position along the conduit.

Equation (1a) describes the evolution of conduit size: $c_1 = 1/(\rho_i L_{lat})$ is a constant that relates the dissipation rate $q\Psi$ to the rate of conduit enlargement through melting. where ρ_i is the density of ice and L_{lat} the specific heat of fusion for ice, while v_o and v_c are functions describing conduit opening due to flow over bed roughness and creep closure, respectively. Wall melt also contributes to water mass balance along the conduit as described by (1b), and r in (1b) is the ratio of ice to water densities, $r = \rho_i/\rho_w$ in order to account for the change in volume on melting. Equation (1c) signifies the generic form of the dependence of discharge on conduit size and hydraulic gradient, while (1d) defines that hydraulic gradient in terms of the effective pressure gradient and a purely geometrical term Ψ_0 : if $b(x)$ and $h(x)$ are bed elevation and ice thickness along the flow path, then

$$\Psi_0 = -\rho_w g \frac{\partial b}{\partial x} - \rho_i g \frac{\partial h}{\partial x}, \quad (2)$$

where g is acceleration due to gravity. As we are interested in lakes that do not require a geometric seal, we do not impose the condition that Ψ_0 change sign along the flow path (Fowler, 1999), and in fact will take Ψ_0 to be a constant for simplicity.

The boundary conditions correspond to a lake at $x = 0$ and the glacier terminus at $x = L$, at which both overburden and water pressure vanish. The left-hand side of (1e) represents the rate of change of water volume stored in the lake basin, while q_{in} is an imposed water input to the lake, which may be constant or vary in time. $V_p = A/(\rho_w g)$ where $A = A(N)$ is the surface area of the lake at the filling level that corresponds to an effective pressure N , given ice overburden $\rho_i g h(0)$ adjacent to the lake. In practice, we will generally treat V_p as a positive constant, idealizing the lake as occupying a vertically-walled basin with constant surface area A .

The model (1) and the model presented in the main paper differ in the retention of the rate of change of conduit cross-section and of the wall melt term in the mass conservation equation (1b). We will demonstrate shortly that these two terms are always small in realistic, terrestrial glacier-dammed lake systems, and can therefore be omitted from the model.

Schoof and others (2014) specifically use the constitutive relations

$$v_o(S) = u_b h_r (1 - S/S_0), \quad v_c(S, N) = c_2 S |N|^{n-1} N, \quad q(S, \Psi) = c_3 S^\alpha |\Psi|^{-1/2} \Psi, \quad (3)$$

where u_b , h_r , S_0 , c_2 , c_3 , n and α are parameters: u_b is sliding velocity and h_r is the amplitude of bed roughness elements and S_0 a cut-off conduit size beyond which bed roughness is drowned out, all assumed to be constant, while c_2 is related to the cross-sectional shape of the conduit and the usual coefficients A and n in Glen's law (Glen, 1958). The exponent $\alpha > 1$ is determined by the choice of turbulent friction parameterization for discharge in the conduit, with $\alpha = 4/3$ for Manning's law and $\alpha = 5/4$ for a Darcy-Weisbach law, and c_3 is similarly determined by the friction law and conduit cross-sectional shape. The notation above in (8a) is almost identical to

that in the corresponding conduit evolution equation in Schoof (2010), except that we have opted here to split the conduit opening term (denoted $v_m(S, \Psi)$ in Schoof (2010)) explicitly into a dissipation-driven melt term $c_1 q \Psi$ and a generic cavity opening term $v_o(S)$.

2.2 Scales and a simplification

We will present results in the main part of this paper in dimensional form. It is however instructive to non-dimensionalize the model in order to simplify the parameter space that needs to be explored, and in order to motivate reducing (1b) to

$$\frac{\partial q}{\partial x} = 0.$$

The contents of this section are not absolutely essential to an understanding of what follows, but will aid in understanding the relationship between the models in sections 2.1 and 2.3, and in how the exploration of parameter space is structured. Put

$$S = [S]S^*, \quad N = [N]N^*, \quad q = [q]q^*, \quad \Psi = [\Psi]\Psi^*, \quad x = [x]x^*, \quad t = [t]t^*$$

where the quantities in square brackets are scales (essentially, a new set of units) that satisfy

$$\frac{[S]}{[t]} = c_1[q] = v_o(0) = v_c([S], [N]), \quad [q] = q([S], \Psi_0), \quad [x] = L. \quad (4)$$

In terms of the dimensionless variables S^* , N^* , q^* , x^* and t^* , the model becomes

$$\frac{\partial S^*}{\partial t^*} = q^* \Psi^* + v_o^*(S^*) - v_c^*(S^*, N^*) \quad (5a)$$

$$\gamma \frac{\partial S^*}{\partial t^*} + \frac{\partial q^*}{\partial x^*} = r \gamma q^* \Psi^* \quad (5b)$$

$$q = q(S, \Psi) \quad (5c)$$

$$\Psi^* = 1 + L^{*-1} \frac{\partial N^*}{\partial x^*} \quad (5d)$$

on $0 < x^* < 1$, subject to boundary conditions

$$-V_p^* \frac{\partial N^*}{\partial t^*} = q_{in}^* - q^* \quad \text{at } x^* = 0 \quad (5e)$$

$$N^* = 0 \quad \text{at } x^* = 1 \quad (5f)$$

with the constitutive equations (3) given by

$$v_o^*(S^*) = 1 - S^*/S_0^*, \quad v_c^*(S^*, N^*) = S^* |N^*|^{n-1} N^*, \quad q^*(S^*, \Psi^*) = S^{*\alpha} |\Psi^*|^{-1/2} \Psi^*. \quad (5g)$$

The dimensionless parameters that remain in the model are

$$r = \frac{\rho_i}{\rho_w}, \quad \gamma = c_1 \Psi_0 L, \quad S_0^* = \frac{S_0}{[S]},$$

$$q_{in}^* = \frac{q_{in}}{c_3[S]^\alpha \Psi_0^{1/2}}, \quad V_p^* = \frac{V_p[N]}{c_3[S]^\alpha \Psi_0^{1/2}[t]}, \quad L^* = \frac{\Psi_0 L}{N}. \quad (6)$$

Since the definitions of the scales $[S]$, $[N]$ and $[t]$ do not involve the values of q_{in} , V_p , L or S_0 , the dimensionless water supply rate q_{in}^* , storage capacity V_p^* , glacier length L^* and conduit cut-off size S_0^* are independent from each other, being direct proxies for their dimensional, unstarred counterparts.

For glacial systems on earth, we can also immediately establish that

$$\gamma \ll 1,$$

and drop the corresponding terms from the model. Specifically, $\Psi_0 L \sim \rho_w g[b] + \rho_i g[h] = \rho_i g(r^{-1}[b] + [h])$ where $[b]$ and $[h]$ are the bed elevation and ice thickness changes along the flow path. Since $c_1 = 1/(\rho_i L_{lat})$, it follows $\gamma = c_1 \Psi_0 L \approx g(r^{-1}[b] + [h])/L_{lat}$ is approximately the ratio of the gravitational potential energy lost by a fixed parcel of water travelling along the flow path to the latent heat of fusion contained in that parcel. With $L_{lat} = 3.35 \times 10^5 \text{ J kg}^{-1}$ and r close to unity, $\gamma \sim O(1)$ would require a total ice surface elevation change $[b] + [h]$ along the flow path of around 33 km, exceeding ice thicknesses on Earth by an order of magnitude. For more typical changes of $[b] + [h] \lesssim 1 \text{ km}$, we find $\gamma \lesssim 3 \times 10^{-2}$, allowing terms of $O(\gamma)$ to be neglected.

As a consequence, we approximate (1b) and (5b) from now on in the form

$$\frac{\partial q}{\partial x} = 0, \quad \frac{\partial q^*}{\partial x^*} = 0, \quad (7)$$

This leaves only q_{in}^* , V_p^* , L^* and S_0^* as dimensionless parameters. S_0^* is essentially a regularizer, intended to stop conduit size from becoming infinite at the glacier terminus, where effective pressure goes to zero and creep closure vanishes as a result. We will use large values of S_0^* (or S_0) throughout the paper, and concentrate on the effect of changes in q_{in}^* , V_p^* , L^* on the dynamics of the drainage system. We ultimately present results in dimensional form in the main paper, and use the dimensional counterparts of these parameters (q_{in} , V_p and L).

2.3 A reduced model

A further simplification is possible if we also deal with a long dimensionless flow path length L^* . By an argument analogous to that in section 2.2, we have $\Psi_0 L \sim \rho_w g[b] + \rho_i g[h]$ and hence large $L^* = (\rho_w g[b] + \rho_i g[h])/[N]$ implies that the hydrostatic drop in pressure over the length of the flow path must be much larger than the typical effective pressure $[N]$. This is realistic in many glacier-dammed lake systems. (Note however that the question of when L^* is large enough for the pressure gradient to be negligible may also depend on the parameters q_{in}^* and V_p^* , since N^* may become large when these other parameters take extreme values. For instance, in section 4 we find an example where we require $L^* \gg V_p^{*(\alpha-1)/(n+1-\alpha)}$ in order for the contribution of pressure to hydraulic to be negligible.)

When $L^* \gg 1$, (5d) and (7) suggest that we can take $q^* \equiv q^*|_{x^*=0}$ and $\Psi_0 = 1$ to be independent of along-flow position x^* (see also Ng, 1998), and reduce the dynamics of the drainage system to two coupled ordinary (rather than partial) differential equations, in dimensional form

$$\dot{S} = c_1 q \Psi + v_o(S) - v_c(S, N) \quad (8a)$$

$$-V_p \dot{N} = q_{in} - q \quad (8b)$$

$$q = q(S, \Psi) \quad (8c)$$

where N is to be understood as $N(0, t)$, the effective pressure at the head of the conduit, at the outlet from the lake, and a dot denotes ordinary differentiation. The constitutive relations can be taken as (3) without modification.

A long flow path $L^* \gg 1$ suggests we put $\Psi^* = 1$, or equivalently $\Psi = \Psi_0$. To retain some representation of the effect of pressure gradients along the flow path, we generalize this in an *ad hoc* fashion to

$$\Psi = \Psi_0 - N/L, \quad (8d)$$

corresponding to a crude divided-difference approximation of the actual gradient $\partial N/\partial x$ by $[N(L, t) - N(0, t)]/L = -N/L$ along the flow path. We will subsequently test the effect of this crude representation against the full, spatially extended model of section 2.1.

A dimensionless version of (8) can be constructed on the basis of the same choice of scales as in section 2.2, and results in (8a) and (8b) taking the form of (5a) and (5e), with the constitutive relations defined through (5g). (8d) simply becomes $\Psi^* = 1 - L^{*-1}N^*$. In the limit of large L^* , we therefore obtain the expected form $\Psi^* = 1$, and the reduced model corresponds to the appropriate limit of the full model.

The reduction of the full model of section 2.1 to a set of ordinary differential equation follows the template of the jökulhlaup model in Ng (1998) and Fowler (1999). The main difference relative to their models is that we allow is for conduits to behave as a cavities due to the opening rate term v_o : the conduit is held open not only by dissipation driven by flow through the conduit, but also by ice flow over basal roughness. This turns out to be key to the limit cycles in our model.

The motivation for using a simpler model is that it allows the theory of dynamical systems (Wiggins, 2003) as well as asymptotic methods to be brought to bear more easily: analysing the reduced model (8) allows us to determine qualitatively not just that limit cycles emerge in particular parameter regimes, but why. This allows us to guide a parallel but more complicated investigation of the full model (1) by purely numerical means.

2.4 A note on lake systems with a seal

As discussed at greater length in the main paper, the model in section 2.1 effectively assumes an ice cliff at $x = 0$, so that effective pressure $N(0, t)$ there can vary in time without causing the ice to detach from the bed and partially floating on the water in

the reservoir. Here we briefly outline the alterations to a one-dimensional model of the form of (1) that are necessary when there is no such cliff, and demonstrate that a seal is then necessary, with $\Psi_0 < 0$ at least close to the reservoir itself.

Let $b(x)$ denote bed elevation, whether this is the lake bed or the base of the glacier, and let $h(x)$ be ice thickness. Assume that part of the lake surface is open to the atmosphere, and let h_w be the elevation of that water surface. Our terminology here differs slightly from that in the main paper (where h_w refers to water level above the lowest point in the lake, whereas we mean water level relative to the same datum as b here).

We assume a shallow glacier geometry and negligible bending moments in the ice (Evatt and Fowler, 2007), so that normal stresses at the base of the ice are cryostatic. Parts of the glacier adjacent to the lake will therefore start to float if $\rho_w g(h_w - b) > \rho_i g h$, and the upstream end of the grounded glacier and the channel inlet can therefore be identified as the location x_f where

$$\rho_w g(h_w - b(x_f)) = \rho_i g h(x_f) \quad (9)$$

With $p_i = \rho_i g h(x_f)$ and $p_w = \rho_w g(h_w - b(x_f))$ at the bed, this of course simply amounts to putting $N(x_f) = p_i = p_w$ at the conduit inlet. As advertised in the main paper, the upstream boundary condition for the lake no longer amounts to specifying a positive N at the conduit inlet as a function of filling level h_w (and hence volume, as we will see shortly) of the lake, but to specifying the inlet location as a function

For a viable lake that will not simply lift ice off the bed near its edge, we require that the ice cannot float, and hence

$$\rho_w g(h_w - b) < \rho_i g h \quad (10)$$

in some finite region adjacent to the lake; this is not quite the hydrological ‘seal’ referred to in the main paper, but closely related to it. With (9), if we assume that x increases in the flow direction of the conduit (i.e., the x -axis points away from the lake and into the glacier at $x = x_f$), this amounts to requiring

$$\frac{\partial[\rho_i g h - \rho_w g(h_w - b)]}{\partial x} > 0 \quad \text{at } x = x_f \quad (11)$$

Since h_w does not depend on x , the left-hand side is of course simply equal to

$$-\Psi_0 = \rho_i g \frac{\partial h}{\partial x} + \rho_w g \frac{\partial b}{\partial x},$$

and this must be positive. In other words, we obtain the rather obvious result that the geometrical hydraulic gradient must be negative and therefore points into the lake: a glacier that partially floats on a lake that it dams must have a ‘seal’ in the sense of a finite region adjacent to the lake where the geometrical hydraulic gradient points into the lake.

We can complete this sketch by relating x_f to lake volume as advertised in the main paper. For a given filling level, (9) specifies where the lake edge is on the glacier

side of the lake. Similarly, the opposite lake edge would be at x_l where $h_w = b(x_l)$, and the volume of the lake can be related to h_w through

$$V = \int_{x_l}^{x_f} h_w - rh(x) - b(x) dx$$

where $h(x) = 0$ in the ice-free parts of the lake, and $r = \rho_i/\rho_w$ as before. With x_l and x_f defined implicitly in terms of h_w , V is clearly a function of h_w alone for a given glacier bed and ice geometry. If we treat this function as invertible, then x_f itself becomes a function of V .

3 Nye's jökulhlaup instability in the reduced model

In this section, we analyze the stability of steady-state solutions to the reduced model (8), following the earlier work of Nye (1976), Ng (1998) and Fowler (1999). Assume quite generally that v_o and v_c satisfy

$$\frac{\partial v_o}{\partial S} \leq 0, \quad \frac{\partial v_c}{\partial S} > 0, \quad \frac{\partial v_c}{\partial N} > 0 \quad (12)$$

with $v_o(S) > 0$ bounded as $S \rightarrow 0$, $v_c(S, 0) = 0$ and $v_c(0, N) = 0$, while q satisfies

$$\frac{\partial q}{\partial S} > 0, \quad \frac{\partial q}{\partial \Psi} > 0. \quad (13)$$

q also has the same sign as $\bar{\Psi}$, and satisfies $q(0, \bar{\Psi}) = q(S, 0) = 0$. These are the minimal assumptions we make on these functions, allowing us to generalize from the specific forms in (3) in analyzing the stability of the drainage system.

The primary dependent variables in the model (8) are S and N . For constant water input q_{in} , the model admits a steady state (\bar{S}, \bar{N}) given implicitly by

$$c_1 q(\bar{S}, \bar{N}) \bar{\Psi} + v_o(\bar{S}) - v_c(\bar{S}, \bar{N}) = 0 \quad (14a)$$

$$q(\bar{S}, \bar{\Psi}) = q_{in} \quad (14b)$$

$$\bar{\Psi} = \Psi_0 - \bar{N}/L. \quad (14c)$$

If $q_{in} > 0$, it follows that $\bar{\Psi} > 0$, and from (14a) and the properties of v_c , we also have $\bar{N} > 0$. For future convenience, we also write $q(\bar{S}, \bar{N}) = \bar{q}$. Note that, for the specific choices in (3), a steady state exists for every positive q_{in} . Eliminating \bar{S} and $\bar{\Psi}$, we find a problem for \bar{N} alone:

$$c_1 q_{in} \left(\Psi_0 - \frac{\bar{N}}{L} \right) + v_o - c_2 \left(\frac{q_{in}}{c_3(\Psi_0 - \bar{N}/L)} \right)^{1/\alpha} \bar{N}^n = 0$$

The left-hand side is a monotonically decreasing function of \bar{N} for $0 \leq \bar{N} < \Psi_0 L$, positive at $\bar{N} = 0$ and tending to $-\infty$ as $\bar{N} \rightarrow \Psi_0 L$, so the equation always admits a unique solution for \bar{N} in this range, from which \bar{S} can then be determined. The solution then has positive \bar{N} , \bar{S} and $\bar{\Psi}$.

We wish to establish conditions under which this steady state is unstable to a Nye-type instability. Previous work due to Ng (1998) and Fowler (1999) indicates that the steady state solution is always unstable for a Manning or Darcy-Weisbach law (3)₃, provided that $v_o = 0$ and $L = \infty$. Here we are interested in the effects of conduit opening due to flow over bed roughness, and the effect of pressure gradients in a system of finite size. Linearizing about the steady state as

$$N = \bar{N} + N', \quad S = \bar{S} + S'$$

and putting $\bar{V}_p = V_p(\bar{N})$ gives

$$\dot{S}' = c_1 q_S \bar{\Psi} S' - (q_\Psi \bar{\Psi} + \bar{q}) L^{-1} N' + v_{o,S} S' - v_{c,S} S' - v_{c,N} N' \quad (15a)$$

$$-\bar{V}_p \dot{N}' = -q_S S' + q_\Psi L^{-1} N' \quad (15b)$$

where

$$q_S = \left. \frac{\partial q}{\partial S} \right|_{S=\bar{S}, \Psi=\bar{\Psi}}, \quad q_\Psi = \left. \frac{\partial q}{\partial \Psi} \right|_{S=\bar{S}, \Psi=\bar{\Psi}}, \quad v_{o,S} = \left. \frac{dv_o}{dS} \right|_{S=\bar{S}},$$

$$v_{c,S} = \left. \frac{\partial v_c}{\partial S} \right|_{S=\bar{S}, N=\bar{N}}, \quad v_{c,N} = \left. \frac{\partial v_c}{\partial N} \right|_{S=\bar{S}, N=\bar{N}}.$$

Looking for solutions of the form $S' = S'_0 \exp(\lambda t)$, $N' = N'_0 \exp(\lambda t)$, we get the eigenvalue problem

$$\begin{pmatrix} c_1 q_S \bar{\Psi} + v_{o,S} - v_{c,S} - \lambda & -c_1 (q_\Psi \bar{\Psi} + \bar{q}) L^{-1} - v_{c,N} \\ \bar{V}_p^{-1} q_S & -\bar{V}_p^{-1} q_\Psi L^{-1} - \lambda \end{pmatrix} \begin{pmatrix} S'_0 \\ N'_0 \end{pmatrix} = 0$$

Setting the determinant of the matrix on the left to zero leads to a polynomial for λ ,

$$\lambda^2 - a_1 \lambda + a_2 = 0 \quad (16)$$

where the coefficients take the form

$$a_1 = c_1 q_S \bar{\Psi} + v_{o,S} - v_{c,S} - \bar{V}_p^{-1} q_\Psi L^{-1} \quad (17a)$$

$$a_2 = \bar{V}_p^{-1} q_S [c_1 (q_\Psi \bar{\Psi} + \bar{q}) L^{-1} + v_{c,N}] - \bar{V}_p^{-1} q_\Psi L^{-1} [c_1 q_S \bar{\Psi} + v_{o,S} - v_{c,S}] \quad (17b)$$

$$= \bar{V}_p^{-1} [c_1 q_S \bar{q} L^{-1} + q_S v_{c,N} + q_\Psi L^{-1} (v_{c,S} - v_{o,S})] \quad (17c)$$

But, from our assumptions on the various functions involved, we see that $a_2 > 0$ (recall that $v_{o,S} \leq 0$ from (12)), while a_1 can be either sign.

The characteristic quadratic (16) has solutions

$$\lambda = \frac{1}{2} \left[a_1 \pm \sqrt{a_1^2 - 4a_2} \right] \quad (18)$$

Since $a_2 > 0$, we have $a_1^2 - 4a_2 < a_1^2$ and two possible types of solution: either $a_1^2 - 4a_2 > 0$ and we have two real roots, both of which have the same sign as a_1 . Alternatively, we have $a_1^2 - 4a_2 < 0$ and a complex conjugate pair of roots, both of

which have real part a_1 . In either case, we see that the system is linearly unstable if and only if $a_1 > 0$, or

$$(c_1 q_S \bar{\Psi} + v_{o,S} - v_{c,S}) - \bar{V}_p^{-1} q_\Psi L^{-1} > 0. \quad (19)$$

We have deliberately written the left-hand side of (19) as the difference of two terms, a potentially destabilizing term $c_1 q_S \bar{\Psi} + v_{o,S} - v_{c,S}$ and a stabilizing term $-\bar{V}_p^{-1} q_\Psi L^{-1}$. As in the main paper, the first term can be recognized as the growth rate for a perturbations to a steady state channel that is kept at a fixed effective pressure. The same term is also the relevant indicator of whether the steady-state conduit is ‘channel-like’ in the terminology of Schoof (2010): in the notation of that paper, we would put $v_m(S, \Psi) = c_1 q(S, \Psi) \Psi + v_o(S)$ so that $\dot{S} = v_m - v_c$. A steady-state conduit is then identified as being channel-like if $v_{m,S} - v_{c,S} > 0$. This criterion here simply becomes

$$v_{m,S} - v_{c,S} = c_1 q_S \bar{\Psi} + v_{o,S} - v_{c,S} > 0. \quad (20)$$

Changing the inequality sign to ‘<’ corresponds to a ‘cavity-like’ conduit, and we see that Nye’s instability will not occur in that case.

Note that the definition of ‘channel-like’ or ‘cavity-like’ in Schoof (2010) distinguishes conduits that are unstable to growth or shrinkage when placed in parallel with a second, identical conduit in the absence of an upstream reservoir from those that are stable when placed in parallel: the former are channels, the latter cavities. The modification of hydraulic gradients to account for gradients in N above notwithstanding, this channelizing instability, described in the supplementary material of Schoof (2010), will still occur if and only they are channel-like as defined by (20). The relevant stability analysis turns out to be identical to that in Schoof (2010).

3.1 Onset of instability under changes in water input

Equation (19) shows that the system experiences Nye’s instability when the conduit is channel-like *and* if the stabilizing effect of increased drainage on effective pressure is not too large. Here, we will show how the instability can be triggered as water input q_{in} to the system is changed. Specifically, we show that for given storage capacity \bar{V}_p and system length L and cavity opening rate $v_o = u_b h$, there is generally a range of intermediate values of q_{in} at which Nye’s instability occurs, if it does at all. Outside of that intermediate range of water inputs, the steady state solution remains stable. Stability at high q_{in} ensured by the effect of limited water storage through the second term in (19), and stability at low q_{in} ensured by a cavity-like conduit through the first term in (19).

Below, we show first that, even with Ψ dependent on N as in (8d), channel- and cavity-like steady states retain the following characteristics demonstrated in Schoof (2010):

$$\frac{d\bar{N}}{dq_{in}} > 0 \quad \text{if channel-like,} \quad \frac{d\bar{N}}{dq_{in}} < 0 \quad \text{if cavity-like} \quad (21)$$

while $d\bar{S}/dq_{in} > 0$ always. Subsequently, we use these properties to show that the conduit switches from cavity-like at small q_{in} to channel-like at large q_{in} at a water input. Nye's instability therefore requires discharge above a critical minimum value.

Next, we show that both, the stabilizing and destabilizing terms in (19) increase with water input q_{in} , but that the stabilizing term does so faster, and hence that Nye's instability is suppressed as a result above an upper critical level of water input: large water throughput makes it harder for water storage to buffer effective pressure against changes due to increased water discharge as conduit size grows. Hence Nye's instability only occurs for an intermediate range of water inputs q_{in} .

It is straightforward to show by applying the chain rule to (14) and rearranging that

$$\frac{d\bar{N}}{dq_{in}} = \frac{c_1 q_S \bar{\Psi} + v_{o,S} - v_{c,S}}{q_S(c_1 q L^{-1} + v_{c,N}) + q_{\Psi} L^{-1}(v_{c,S} - v_{o,S})}, \quad (22a)$$

$$\frac{d\bar{S}}{dq_{in}} = \frac{c_1(q_{\Psi} \bar{\Psi} + q)L^{-1} + v_{c,N}}{q_S(c_1 q L^{-1} + v_{c,N}) + q_{\Psi} L^{-1}(v_{c,S} - v_{o,S})}, \quad (22b)$$

where, with the constraints in (12), we see that $d\bar{N}/dq_{in}$ is the same sign as $q_S \bar{\Psi} + v_{o,S} - v_{c,S}$, while $d\bar{S}/dq_{in} > 0$ always. As in the simpler model in Schoof (2010), effective pressure increases with water input in the channel-like state, while it decreases in the cavity-like state. Conduit cross-section always increases with water input.

We can also show that the conduit must be cavity-like at low q_{in} . Note that $\bar{\Psi}$ must lie between 0 and Ψ_0 . Since $\bar{\Psi}$ is therefore bounded, the term $q(\bar{S}, \bar{N})\bar{\Psi} = q_{in}\bar{\Psi}$ in (14a) approaches zero at low q_{in} , while $v_o(\bar{S})$ remains bounded below (and in fact approaches a constant value). Hence we must have $v_o(\bar{S}) \sim v_c(\bar{S}, \bar{N})$. It is easy to show then that \bar{N} decreases with \bar{S} : with (3), we have $\bar{N}^n \sim u_b h / (c_2 \bar{S})$ as in Schoof (2010). More generally, by the chain rule

$$\frac{d\bar{N}}{dq_{in}} \sim \frac{v_{o,S} - v_{c,S}}{v_{c,N}} \frac{d\bar{S}}{dq_{in}}$$

Since $d\bar{S}/dq_{in} > 0$ and $v_{o,S} < 0$, $v_{c,S} > 0$, it follows that \bar{N} decreases with increasing q_{in} at low q_{in} , and the conduit is therefore cavity-like and stable at low water input.

Conversely, at high water input, it can be shown with (3) that the conduit must be channel-like. It is straightforward to see that (14a) reduces to $c_1 q_{in} \bar{\Psi} \sim c_2 \bar{S} \bar{N}^n$ with $\bar{N} \sim \Psi_0 L$. We also have $q_{in} = c_3 \bar{S}^\alpha \bar{\Psi}^{1/2}$, and hence $\bar{S} \sim [c_1 / (c_2 c_3^2)]^{1/(2\alpha+1)} q_{in}^{3/(2\alpha+1)} (\Psi_0 L)^{n/(2\alpha+1)}$. But $N = L[\Psi_0 - \bar{\Psi}] = L[\Psi_0 - q_{in}^2 / (c_3^2 S^{2\alpha})]$ so

$$N \sim L \left[\Psi_0 - c_3^{-2/(2\alpha+1)} (c_2/c_1)^{2\alpha/(2\alpha+1)} (\Psi_0 L)^{2n\alpha/(2\alpha+1)} q_{in}^{-2(\alpha-1)/(2\alpha+1)} \right],$$

and N decreases with q_{in} at large q_{in} , so the conduit is channel-like.

Next we show that the system can change from cavity-like to channel-like only once as q_{in} increases, so there is a single critical water input at which this switch must happen. Consider differentiating the measure $c_1 q_S \bar{\Psi} + v_{o,S} - v_{c,S}$ of 'channel-likeness'

with respect to q_{in} . We have

$$\frac{d(c_1 q_S \bar{\Psi} + v_{o,S} - v_{c,S})}{dq_{in}} = (c_1 q_{SS} \bar{\Psi} + v_{o,SS} - v_{c,SS}) \frac{d\bar{S}}{dq_{in}} - (c_1 (q_{S\Psi} \bar{\Psi} + q_S) L^{-1} + v_{c,SN}) \frac{d\bar{N}}{dq_{in}}, \quad (23)$$

with $q_{SS} = \partial^2 q / \partial S^2|_{S=\bar{S}, N=\bar{N}}$ etc. Note that, from (3), we have $q_{SS} \bar{\Psi} + v_{o,SS} - v_{c,SS} > 0$ as well as $q_{S\Psi} > 0$, $v_{c,SN} > 0$. From (22a), the right-hand side of (23) is positive whenever the conduit is cavity-like with $q_S \bar{\Psi} + v_{o,S} - v_{c,S} < 0$. It follows that $q_S \bar{\Psi} + v_{o,S} - v_{c,S}$ can only ever change sign from negative to positive as q_{in} increases. There is therefore a single value of q_{in} at which the conduit changes from cavity-like to channel-like. Nye's instability can only occur above this critical value.

We can also show that the second, stabilizing term in (19) becomes dominant at large water inputs. With (3) and (14a), we have

$$c_2 \bar{N}^n = c_1 c_3 \bar{S}^{\alpha-1} \bar{\Psi}^{3/2} + \frac{u_b h_r (1 - S/S_0)}{\bar{S}}$$

and hence

$$\begin{aligned} c_1 q_S \bar{\Psi} + v_{o,S} - v_{c,S} &= (\alpha - 1) c_1 c_3 \bar{S}^{\alpha-1} \bar{\Psi}^{3/2} - \frac{u_b h_r}{\bar{S}} \\ &= \frac{(\alpha - 1) c_1 q_{in} \bar{\Psi}}{\bar{S}} - \frac{u_b h}{\bar{S}} \end{aligned} \quad (24)$$

while

$$\begin{aligned} \bar{V}_p^{-1} q_\Psi L^{-1} &= \frac{c_3 S^\alpha}{2 \bar{V}_p L \bar{\Psi}^{1/2}} \\ &= \frac{c_3}{2 \bar{V}_p L} \frac{q_{in}}{\bar{\Psi}} \end{aligned} \quad (25)$$

so that

$$(c_1 q_S \bar{\Psi} + v_{o,S} - v_{c,S}) - \bar{V}_p^{-1} q_\Psi L^{-1} = \frac{c_1 q_{in}}{\bar{\Psi}} \left(\frac{(\alpha - 1) \bar{\Psi}^2}{\bar{S}} - \frac{c_3}{2 c_1 \bar{V}_p L} - \frac{u_b h \bar{\Psi}}{c_1 q_{in} \bar{S}} \right) \quad (26)$$

But, from the above, we know that \bar{N} increases monotonically with q_{in} when q_{in} is above the critical value for channel-like behaviour. In that regime, $\bar{\Psi} = \Psi_0 - \bar{N}/L$ therefore decreases with q_{in} . At the same time \bar{S} increases with q_{in} ; in fact, since $\bar{S} = q_{in}^{1/\alpha} / \bar{\Psi}^{1/(2\alpha)}$, \bar{S} increases without bound. It is therefore clear that the bracketed term on the right-hand side of (26) becomes negative for sufficiently large q_{in} , and that Nye's instability is suppressed by large water inputs.

Combined, these results show that Nye's instability can only occur when q_{in} is large enough for the conduit to be channel-like, but not large enough for the stabilizing effect of limited water storage to dominate.

The existence of such an unstable range of values of q_{in} is, however, not guaranteed for given values of the remaining parameters. Recall that the steady state solution (\bar{S}, \bar{N}) does not depend on the value of \bar{V}_p , and hence so are the coefficients q_S , $v_{o,S}$,

$v_{c,S}$, q_Ψ and $\bar{\Psi}$ in (26). Changes in storage capacity \bar{V}_p therefore affect stability purely through that second term in (26): making \bar{V}_p small enough while keeping all other parameters constant will increase the size of the stabilizing term to any value required while keeping the destabilizing term constant. Given that we have just shown that there is only ever a finite range of q_{in} over which instability will occur for a given \bar{V}_p , the size of the destabilizing term over that range for one value of \bar{V}_p is bounded, and it follows that we make the system stable for all values of q_{in} within that range by simply shrinking \bar{V}_p enough. Conversely, by making $\bar{V}_p \rightarrow \infty$, we can make the stabilizing term vanish, and ensure that instability occurs. In other words, for fixed values of all the other parameters, a minimum value of \bar{V}_p is required to cause Nye's instability to occur in practice.

3.2 Computing the stability boundary

In the main paper, we plot stability boundaries for the model (8) as curves of points (q_{in}, \bar{V}_p) for fixed L at which a change from a stable to an unstable steady state occurs, demarcating regions in parameter space where we expect instability to occur: steady drainage of the lake will not persist in these unstable regions, and we expect outburst floods will occur. Computing these stability boundaries amounts finding combinations $(\bar{S}, \bar{N}, q_{in}, \bar{V}_p)$ of the system

$$q(\bar{S}, \Psi_0 - \bar{N}/L) = q_{in} \quad (27a)$$

$$c_1 q(\bar{S}, \Psi_0 - \bar{N}/L)(\Psi_0 - \bar{N}/L) + v_o(\bar{S}) - v_c(\bar{S}, \bar{N}) = 0 \quad (27b)$$

$$c_1 q_S(\bar{S}, \Psi_0 - \bar{N}/L) + v_{o,S}(\bar{S}) - v_{c,S}(\bar{S}, \bar{N}) - \bar{V}_p^{-1} q_\Psi(\bar{S}, \Psi_0 - \bar{N}/L) L^{-1} = 0 \quad (27c)$$

for a given set of the remaining parameters; given these three equations for the for unknowns $(\bar{S}, \bar{N}, q_{in}, \bar{V}_p)$, the problem defines a one-dimensional curve in a four-dimensional space.

We solve the problem numerically using arc length continuation based on Newton's method. Generically, let $f : \mathbb{R}^n \times \mathbb{R} \mapsto \mathbb{R}^n$ and assume we are solving a rootfinding problem $f(z; \mu) = 0$ for an n -dimensional vector-valued variable z given a parameter μ . The continuation method then works as follows: given a solution $(z_i; \mu_i)$, we find a new solution solution (z_{i+1}, μ_{i+1}) defined by

$$f(z_{i+1}, \mu_{i+1}) = 0, \quad d(\mu_{i+1}, \mu_i) = s \quad (28)$$

where s is a prescribed positive value and d is a distance metric. This in itself becomes an $(n+1)$ -dimensional rootfinding problem in which μ_{i+1} is part of the solution, and can be solved using Newton's method. Here of course $z = (\bar{S}, \bar{N}, q_{in})$ and $\mu = \bar{V}_p$ or $z = (\bar{S}, \bar{N}, \bar{V}_p)$ and $\mu = q_{in}$.

Asymptotic forms of the stability boundary are relatively straightforward to derive when L is large. For large L and $\bar{V}_p \sim O(1)$ or large, it is straightforward to show that one solution to

$$c_1 q_S(\bar{S}, \Psi_0 - \bar{N}/L) + v_{o,S}(\bar{S}) - v_{c,S}(\bar{S}, \bar{N}) - \bar{V}_p^{-1} q_\Psi(\bar{S}, \Psi_0 - \bar{N}/L) L^{-1} = 0$$

can be approximated by omitting the second, stabilizing term, since this behaves as $\sim (\bar{V}_p L)^{-1}$. With L large, we also have $\Psi_0 - \bar{N}/L \sim \Psi_0$, and the stability boundary is given by

$$c_1 q_S(\bar{S}, \Psi_0) + v_{o,S}(\bar{S}) - v_{c,S}(\bar{S}, \bar{N}) \sim 0;$$

this is simultaneously the boundary of ‘channel-like’ conduit behaviour. If we assume the constitutive relations in (3) with large S_0 (so $v_{o,S} = 0$), this boundary is at

$$\bar{S} = \left(\frac{u_b h_r}{(\alpha - 1) c_1 c_3 \Psi_0} \right)^{1/\alpha}, \quad \bar{N} = \left(\frac{\alpha c_1 \bar{S}^{\alpha-1} \Psi_0}{c_2} \right)^{1/n}, \quad q_{in} = \frac{u_b h_r}{(\alpha - 1) c_1 \Psi_0}. \quad (29)$$

This can be refined for large \bar{V}_p and finite L , in which case Ψ can no longer be approximated accurately by Ψ_0 : in the first two equalities in (29), Ψ_0 then needs to be replaced by $\Psi_0 = \bar{N}/L$, and together the two form equations that must be solved numerically for \bar{S} and \bar{N} . Given a result for \bar{N} , Ψ_0 in the third equality for the critical value of q_{in} also needs to be replaced by $\Psi_0 - \bar{N}/L$. The corrected critical value will be somewhat larger than that given in (29).

Equation (29)₃ is an asymptotic formula for the lower value of water supply at which steady drainage becomes unstable. Recall that in general a finite band of values of q_{in} is unstable. We can also find an asymptotic formula for the larger critical value, at which steady drainage becomes stable again. Assume again that L and \bar{V}_p are large. In order for the second, stabilizing term in (27c) to balance the first, discharge q_{in} and conduit size \bar{S} must be large, since only in that case can $\bar{V}_p^{-1} L^{-1} q_\psi = q_{in}/(2\bar{V}_p \bar{\Psi} L) \sim q_{in}/(2\bar{V}_p \Psi_0 L)$ be comparable to $q_S = \alpha q_{in}/\bar{S}$. For such large discharges, the conduit acts entirely channel-like, and at leading order $|\bar{N}|^{n-1} \bar{N} \sim c_1 c_3 \bar{S}^{\alpha-1} \Psi_0^{3/2}/c_2$, so

$$c_1 q_S(\bar{S}, \Psi_0) + v_{o,S}(\bar{S}) - v_{c,S}(\bar{S}, \bar{N}) \sim c_1 c_3 \bar{S}^{\alpha-1} \Psi_0^{3/2}$$

Equating this with $\bar{V}_p^{-1} q_\psi L^{-1} \sim \bar{V}_p^{-1} q_{in} \Psi_0^{-1} L^{-1}/2$ and using $q_{in} \sim c_3 \bar{S}^\alpha \Psi_0^{1/2}$, the stability boundary is at

$$\bar{V}_p \sim \frac{q_{in}^{1/\alpha}}{2(\alpha - 1) c_1 c_3^{1/\alpha} \Psi_0^{(3\alpha+2)/(2\alpha)} L}. \quad (30)$$

3.3 Weakly nonlinear stability analysis

The change from a stable to an unstable steady state, for instance under changes in q_{in} as in section 3.1, occurs when the real part of at least one of the eigenvalues λ changes from negative to positive. While the preceding section provides a means of computing where the onset of instability occurs, it does not offer information on where the unstable evolution of solutions leads to. A weakly nonlinear stability analysis provides some of that information.

From the discussion following (18), the onset of instability corresponds to $a_1 = 0$ and hence to $\lambda = \pm i\sqrt{a_2}$. A change from stability to instability at which two eigenvalues are purely imaginary is termed a Hopf bifurcation (Wiggins, 2003). This type

of bifurcation leads to the generation of a limit cycle solution that oscillates around the steady state solution, with an amplitude that goes to zero at the bifurcation point itself. This limit cycle solution can come in two flavours: either it is a stable limit cycle that exists around the unstable branch of the steady state solution (the bifurcation is then known as a supercritical Hopf bifurcation), or it is an unstable closed orbit around the stable steady state solution (a subcritical Hopf bifurcation).

If the bifurcation is supercritical, then the onset of instability leads to stable, small-scale oscillations that grow in amplitude as the bifurcation parameter q_{in} moves away from its critical value at which the change from stability to instability occurs. If the bifurcation is subcritical, this is not the case, and different behaviour (such as a limit cycle with large amplitude) must emerge. Here we lay out the machinery for determining whether the bifurcation is sub- or supercritical, which (given the nature of the algebraic manipulations required) is then done numerically as in the main part of the paper. What follows is standard procedure, and we include it here for completeness.

Generically, we consider a 2-dimensional autonomous dynamical system that depends on a parameters μ ,

$$\frac{dy_i}{dt} = F_i(y; \mu), \quad (31)$$

and which admits a steady state $F_i(y_i^{(0)}, \mu_0) = 0$ and where F is real-valued for real y and μ , and sufficiently smooth around that steady state. Let

$$F_{i,jkl\dots} = \left. \frac{\partial^n F_i}{\partial y_j \partial y_k \partial y_l \dots} \right|_{y=y^{(0)}, \mu=\mu_0}.$$

The equilibrium solution $y^{(0)}$ at $\mu = \mu_0$ corresponds to a Hopf bifurcation if the Jacobian matrix $F_{i,j}$ has a pair of purely imaginary eigenvalues $\pm i\omega$, which we assume to be the case. We also define

$$F_{i,\mu} = \left. \frac{\partial F_i}{\partial \mu} \right|_{y=y^{(0)}, \mu=\mu_0}, \quad F_{i,j\mu} = \left. \frac{\partial^2 F_i}{\partial y_j \partial \mu} \right|_{y=y^{(0)}, \mu=\mu_0}$$

We simultaneously perturb $y^{(0)}$ and μ as

$$y = y^{(0)} + \varepsilon y^{(1)} + \varepsilon^2 y^{(2)} + \varepsilon^3 y^{(3)} + o(\varepsilon^3), \quad \mu = \mu^{(0)} \pm \varepsilon^2,$$

where ε is some small number, and introduce a slow time variable T in addition to t through

$$T = \varepsilon^2 t.$$

Treating T and t as independent variables as in a multiple scales expansion (Holmes,

1995), we get

$$\begin{aligned}
\varepsilon \frac{\partial y_i^{(1)}}{\partial t} + \varepsilon^2 \frac{\partial y_i^{(2)}}{\partial t} + \varepsilon^3 \frac{\partial y_i^{(3)}}{\partial t} + \varepsilon^3 \frac{\partial y_i^{(1)}}{\partial T} &= F_{i,j} \left(\varepsilon y_j^{(1)} + \varepsilon^2 y_j^{(2)} + \varepsilon^3 y_j^{(3)} \right) \\
&+ \frac{1}{2} F_{i,jk} \left(\varepsilon y_j^{(1)} + \varepsilon^2 y_j^{(2)} + \varepsilon^3 y_j^{(3)} \right) \left(\varepsilon y_k^{(1)} + \varepsilon^2 y_k^{(2)} + \varepsilon^3 y_k^{(3)} \right) \\
&+ \frac{1}{6} F_{i,jkl} \left(\varepsilon y_j^{(1)} + \varepsilon^2 y_j^{(2)} + \varepsilon^3 y_j^{(3)} \right) \left(\varepsilon y_k^{(1)} + \varepsilon^2 y_k^{(2)} + \varepsilon^3 y_k^{(3)} \right) \\
&\times \left(\varepsilon y_l^{(1)} + \varepsilon^2 y_l^{(2)} + \varepsilon^3 y_l^{(3)} \right) \pm \varepsilon^2 F_{i,\mu} \pm \varepsilon^3 F_{i,j\mu} y_j^{(1)} + o(\varepsilon^3)
\end{aligned} \tag{32}$$

where we have used the summation convention for repeated indices, and the sign in ‘ \pm ’ has to be picked consistently between the two uses of that symbol. Equating powers of ε ,

$$\frac{\partial y_i^{(1)}}{\partial t} = F_{i,j} y_j^{(1)} \tag{33}$$

$$\frac{\partial y_i^{(2)}}{\partial t} = F_{i,j} y_j^{(2)} + \frac{1}{2} F_{i,jk} y_j^{(1)} y_k^{(1)} \pm F_{i,\mu} \tag{34}$$

$$\begin{aligned}
\frac{\partial y_i^{(3)}}{\partial t} + \frac{\partial y_i^{(1)}}{\partial T} &= F_{i,j} y_j^{(3)} + \frac{1}{2} F_{i,jk} \left(y_j^{(1)} y_k^{(2)} + y_j^{(2)} y_k^{(1)} \right) + \frac{1}{6} F_{i,jkl} y_j^{(1)} y_k^{(1)} y_l^{(1)} \pm F_{i,j\mu} y_j^{(1)} \\
&= F_{i,j} y_j^{(3)} + F_{i,jk} y_j^{(1)} y_k^{(2)} + \frac{1}{6} F_{i,jkl} y_j^{(1)} y_k^{(1)} y_l^{(1)} \pm F_{i,j\mu} y_j^{(1)}
\end{aligned} \tag{35}$$

With $F_{i,j}$ having imaginary, conjugate eigenvalues $\pm i\omega$, we get

$$y_i^{(1)} = A(T) e_i \exp(i\omega t) + \overline{A(T)} \overline{e_i} \exp(-i\omega t) \tag{36}$$

where e_i is the eigenvector of $F_{i,j}$ corresponding to the eigenvalue $i\omega$, and $A(T)$ is a potentially complex amplitude. An overbar denotes complex conjugation.

At second order, we get

$$\begin{aligned}
\frac{\partial y_i^{(2)}}{\partial t} - F_{i,j} y_j^{(2)} &= \frac{1}{2} F_{i,jk} e_j e_k A(T)^2 \exp(2i\omega t) + \frac{1}{2} F_{i,jk} \overline{e_j} \overline{e_k} \overline{A(T)}^2 \exp(-2i\omega t) \\
&+ \frac{1}{2} F_{i,jk} (e_j \overline{e_k} + \overline{e_j} e_k) |A(T)|^2 \pm F_{i,\mu}
\end{aligned} \tag{37}$$

where, by symmetry, $(1/2) F_{i,jk} (e_j \overline{e_k} + \overline{e_j} e_k) = F_{i,jk} e_j \overline{e_k}$. This has solution

$$y_i^{(2)} = B e_i \exp(i\omega t) + \overline{B} \overline{e_i} \exp(-i\omega t) \tag{38}$$

$$+ (2i\omega \delta_{ij} - F_{i,j})^{-1} \frac{1}{2} F_{j,kl} e_k e_l A(T)^2 \exp(2i\omega t) \tag{39}$$

$$+ (-2i\omega \delta_{ij} - F_{i,j})^{-1} \frac{1}{2} F_{j,kl} \overline{e_k} \overline{e_l} \overline{A(T)}^2 \exp(-2i\omega t) \tag{40}$$

$$- F_{i,j}^{-1} (F_{j,kl} e_k \overline{e_l} |A(T)|^2 \pm F_{j,\mu}), \tag{41}$$

where B is again a potentially complex amplitude (dependent on T , though this will be immaterial below), and δ_{ij} is the Kronecker delta. The notation A_{ij}^{-1} indicates the ij -component of the matrix inverse of A_{ij} .

At third order, we have a problem of the form

$$\frac{\partial y_i^{(3)}}{\partial t} - F_{i,j} y_j^{(3)} = c_i \exp(i\omega t) + d_i \exp(i3\omega t) + \bar{c}_i \exp(-i\omega t) + \bar{d}_i \exp(i3\omega t) \quad (42)$$

with

$$\begin{aligned} c_i(T) &= F_{i,jk} (2i\omega\delta_{jl} - F_{j,l})^{-1} \frac{1}{2} F_{l,mn} e_m e_n \bar{e}_k |A(T)|^2 A(T) \\ &\quad - F_{i,jk} F_{j,l}^{-1} (F_{l,mn} e_m \bar{e}_n |A(T)|^2 \pm F_{l,\mu}) e_k A(T) \\ &\quad + \frac{1}{2} F_{i,jkl} e_j e_k \bar{e}_l |A(T)|^2 A(T) \\ &\quad \pm F_{i,j\mu} e_j A(T) - \frac{\partial A}{\partial T} e_i \end{aligned} \quad (43)$$

We have only written out explicitly the coefficient of $\exp(i\omega t)$ but not that of $\exp(i3\omega t)$. The crucial point about having a term proportional to $\exp(i\omega t)$ on the right-hand side of (43) is that this term is resonant, and potentially leads to secular growth in $y_i^{(3)}$ because $i\omega$ is one of the eigenvalues of $F_{i,j}$, whereas a term proportional to $\exp(i3\omega t)$ will not. By the Fredholm alternative, a bounded solution exists if and only if

$$c_i v_i = 0$$

where v_i is the right eigenvector corresponding to the eigenvalue $i\omega$, i.e. v_i is a non-trivial vector satisfying $v_i (F_{i,j} - i\omega\delta_{ij}) = 0$.

This leads to the Landau equation, of the form

$$\frac{\partial A}{\partial T} + aA + b|A|^2 A = 0 \quad (44)$$

with

$$a = \pm (F_{i,jk} F_{j,l}^{-1} F_{l,\mu} e_k v_i - F_{i,j\mu} e_j v_i) / e_l v_l \quad (45)$$

$$b = \left[F_{i,jk} F_{j,l}^{-1} F_{l,mn} e_k e_m \bar{e}_n - F_{i,jk} (2i\omega\delta_{jl} - F_{j,l})^{-1} \frac{1}{2} F_{l,mn} e_m e_n \bar{e}_k - \frac{1}{2} F_{i,jkl} e_j e_k \bar{e}_l \right] v_i / e_p v_p \quad (46)$$

A supercritical Hopf bifurcation corresponds to the real part of b being positive, while the real part of b being negative signals a subcritical bifurcation: Multiplying (44) by \bar{A} and adding the resulting equation to its own complex conjugate, we obtain

$$\frac{\partial |A|^2}{\partial T} + \Re(a) |A|^2 + \Re(b) |A|^4 = 0.$$

Growth occurs when $\Re(a) < 0$ (which can be toggled by choice of the sign of the perturbation in ‘ \pm ’), and remains bounded if $\Re(b) > 0$, in which case $|A|^2$ saturates at a values of $-\Re(a)/\Re(b)$.

Let $S = y_1$, $N = y_2$, $\mu = q_{in}$, and consider the dynamical system (8) with (3) and V_p constant. Then the non-zero derivative terms for the dynamical system (8) are

$$\begin{aligned}
F_{1,1} &= c_1 q_S \Psi - v_{c,S}, & F_{1,2} &= -c_1 (q_\Psi \Psi + q) L^{-1} - v_{c,N}, & F_{2,1} &= \bar{V}_p^{-1} q_S, & F_{2,2} &= -\bar{V}_p^{-1} q_\Psi L^{-1}, \\
F_{1,11} &= c_1 q_{SS} \Psi, & F_{1,12} &= F_{1,21} = -c_1 (q_{S\Psi} \Psi + q_S) L^{-1} - v_{c,SN}, & F_{1,22} &= c_1 (q_{\Psi\Psi} \Psi + 2q_\Psi) L^{-2} - v_{c,NN}, \\
F_{2,11} &= \bar{V}_p^{-1} q_{SS}, & F_{2,12} &= F_{2,21} = -\bar{V}_p^{-1} q_{S\Psi} L^{-1}, & F_{2,22} &= \bar{V}_p^{-1} q_{\Psi\Psi} L^{-2}, \\
F_{1,111} &= c_1 q_{SSS} \Psi, & F_{1,112} &= F_{1,121} = F_{1,211} = -c_1 (q_{SS\Psi} \Psi + q_{SS}) L^{-1}, \\
F_{1,122} &= F_{1,212} = F_{1,221} = c_1 (q_{S\Psi\Psi} \Psi + 2q_{S\Psi}) L^{-2} - v_{c,SNN}, & F_{1,222} &= -c_1 (q_{\Psi\Psi\Psi} \Psi + 3q_{\Psi\Psi}) L^{-3} - v_{c,NNN}, \\
F_{2,111} &= \bar{V}_p^{-1} q_{SSS}, & F_{2,112} &= F_{2,121} = F_{2,211} = -\bar{V}_p^{-1} q_{SS\Psi} L^{-1}, \\
F_{2,122} &= F_{2,212} = F_{2,221} = \bar{V}_p^{-1} q_{S\Psi\Psi} L^{-2} & F_{2,222} &= -\bar{V}_p^{-1} q_{\Psi\Psi\Psi} L^{-3};
\end{aligned}$$

This allows the Landau coefficients $\Re(a)$ and $\Re(b)$ to be computed directly. We do this numerically (by simple function evaluation) at the same time as computing the location of the stability boundaries, allowing us to identify whether the bifurcations at these boundaries are super- or sub-critical.

3.4 Numerical computation of closed orbits and their stability: bifurcation diagrams

The results of the previous section allow us to determine whether the Hopf bifurcation leads locally to a stable limit cycle or not, but does not allow us to trace the evolution of closed orbits as parameter values are changed. This can only be done numerically.

A closed orbit corresponds to a fixed point of the Poincaré map of the dynamical system (8), defined as the discrete mapping that maps one intersection of an orbit of the dynamical system with a transversal hypersurface to the next such intersection (Wiggins, 2003). This section describes the basics behind the computational method used to compute closed orbits as fixed points of the Poincaré map, and to determine whether the closed orbits are stable. Again, the method is a standard technique that is included for completeness here. In practice, we use the nullclines of the dynamical system (the hypersurfaces on which either \dot{S} or \dot{N} are zero) as the relevant transversal hypersurfaces. By using the N -nullcline, this further allows us to identify the minimum and maximum of N along each closed orbit.

The method we use to find fixed points of the Poincaré map is a single shooting method. This becomes unsuitable for certain extreme parameter combinations, but has the advantage of being easily implemented and of computing the Jacobian of the map automatically, allowing the stability of the map (and hence of the closed orbits) to be determined immediately. Assume again that we write the dynamical system as

$$\frac{dy}{dt} = F(y; \mu), \quad (47)$$

with a solution $y = Y(t; \mu, y_0)$ that depends on time t , the parameter μ and the initial condition y_0 , with $Y(0; \mu, y_0) = y_0$.

In our case, we integrate up to a nullcline, or more generally, a transversal hyper-surface defined by $g(y; \mu) = 0$ where g is scalar-valued. In other words, we need to evaluate $Y(t_f; \mu, y_0)$ at the time t_f at which

$$g(Y(t_f; \mu, y_0); \mu) = 0,$$

which numerical initial value problem solvers are generally able to; g is then known as an ‘event function’. This condition also implicitly defines the final time t_f as a function of y_0 and μ . The problem of finding a closed orbit then amounts to finding y_0 such that

$$Y(t_f(\mu, y_0); \mu, y_0) - y_0 = 0 \tag{48}$$

Solving this by using Newton’s method requires us to compute the gradient of the left-hand side with respect to y_0 .

To avoid notational tangles, define a new function

$$\mathcal{Y}(\mu, y_0) = Y(t_f(\mu, y_0); \mu, y_0).$$

As in a standard shooting method (Atkinson, 1989), we can define the gradient of the fixed-time solution $Y(t; \mu, y_0)$ with respect to y_0 . Again, for later notational simplicity, put

$$J_{ij}(t; \mu, y_0) = \left. \frac{\partial Y_i}{\partial y_{0,j}} \right|_{(t; \mu, y_0)}$$

This gradient satisfies the linear differential equation

$$\frac{dJ_{ij}}{dt} = \left. \frac{\partial F_i}{\partial y_k} \right|_{(Y(t; \mu, y_0); \mu)} J_{kj}, \tag{49}$$

subject to

$$J_{kj}(0; \mu, y_0) = \delta_{kj}.$$

Note that $\partial F_i / \partial y_k$ is a function of Y and μ but not of the gradient J (hence the linearity of the equation). This equation is straightforward to integrate numerically. We still need to account for the dependence of t_f on y_0 in order to compute the gradient of \mathcal{Y} rather than Y : we have

$$\frac{\partial \mathcal{Y}_i}{\partial y_{0,j}} = J_{ij}(t_f; \mu, y_0) + F_i(\mathcal{Y}(\mu, y_0); \mu) \frac{\partial t_f}{\partial y_{0,j}}$$

For further simplicity, put

$$n_j = \left. \frac{\partial g}{\partial Y_j} \right|_{(\mathcal{Y}(\mu, y_0); \mu)}$$

Using the implicit definition of t_f , we have by the chain rule

$$\begin{aligned} 0 &= \frac{\partial g(Y(t_f(\mu, y_0); \mu, y_0))}{\partial y_{0,j}} \\ &= n_k F_k(\mathcal{Y}(\mu, y_0); \mu) \frac{\partial t_f}{\partial y_{0,i}} + n_l J_{lj}(t_f; \mu, y_0) \end{aligned}$$

or

$$\frac{\partial t_f}{\partial y_{0,j}} = -\frac{n_l J_{lj}(t_f; \mu, y_0)}{n_k F_k(\mathcal{Y}(\mu, y_0); \mu)};$$

once the orbit from y_0 to its intersection point $\mathcal{Y}(\mu, y_0)$ has been computed, this suffices to then determine $\partial \mathcal{Y}_i / \partial y_{0,j}$ and apply Newton's method to finding roots of (48),

$$\frac{\partial \mathcal{Y}_i}{\partial y_{0,j}} = \left(\delta_{il} - \frac{F_i n_l}{n_k F_k} \right) J_{lj}, \quad (50)$$

where all terms on the right-hand side are evaluated at $t = t_f(\mu, y_0)$, $y = Y(t_f(\mu, y_0); \mu, y_0) = \mathcal{Y}(\mu, y_0)$.

Note that $y_0 \mapsto \mathcal{Y}(\mu, y_0)$ is not the Poincaré map per se; this is only true for the restriction of \mathcal{Y} to arguments y_0 that themselves lie on the transversal surface defined by $g = 0$. Finding roots of (48) naturally ensures that the root y_0 itself lies on that transversal surface. This observation is however relevant to finding the Jacobian of the Poincaré map, which allows us to determine the stability of closed orbits: the latter are stable if the spectral radius of that Jacobian is less than unity, and unstable if the greater than unity.

It is straightforward to show that all but one of the right eigenvectors of $\partial \mathcal{Y}_i / \partial y_{0,j}$ lie in the tangent plane to the surface $g = 0$, and are therefore eigenvectors of the Poincaré map. The additional eigenvector that does not lie in the tangent plane has zero eigenvalue and therefore does not affect the spectral radius. To show this, it suffices to recognize that n_i is a left eigenvector of $\partial \mathcal{Y}_i / \partial y_{0,j}$ with zero eigenvalue,

$$n_i \frac{\partial \mathcal{Y}_i}{\partial y_{0,j}} = n_i \left(\delta_{il} - \frac{F_i n_l}{n_k F_k} \right) J_{lj} = 0,$$

and that right eigenvectors are then either perpendicular to n_i , or themselves have zero eigenvalue. Assuming that J is invertible, the multiplicity of the zero eigenvalue is one, and the corresponding right eigenvector can be written as $e_i = J_{ij}^{-1} F_j$. The remaining eigenvectors are therefore normal to n_i ; since n_i is the gradient of g , this implies that these eigenvectors lie in the tangent plane to $g = 0$ as required. In other words, the spectral radius of the Jacobian $\partial \mathcal{Y}_i / \partial y_{0,j}$ is the spectral radius of the Jacobian of the Poincaré map itself.

Computationally, we solve (47) and (49) for \mathcal{Y} and J_{ij} using inbuilt MATLAB initial value solvers (usually ode15s, since the system becomes stiff when the lake storage capacity is large, as is often of interest), and use (50). This allows us to solve (48) by Newton's method, with an arc length continuation method allowing us to trace the evolution of closed orbits under parameter changes. This follows the scheme of (28), with $f(y_0, \mu) = \mathcal{Y}(\mu, y_0) - y_0$. Applying Newton's method to the arc length continuation scheme requires the derivative of \mathcal{Y} with respect to μ . This can be computed by analogy with the method above.

Let $Y_{i,\mu} = \frac{\partial Y_i}{\partial \mu}$; $Y_{i,\mu}$ satisfies

$$\frac{dY_{i,\mu}}{dt} = \frac{\partial F_i}{\partial y_k} \Big|_{(Y(t;\mu,y_0);\mu)} Y_{k,\mu} + \frac{\partial F_i}{\partial \mu} \Big|_{(Y(t;\mu,y_0);\mu)} Y_{k,\mu}$$

subject to $Y_{i,\mu}(0; \mu, y_0) = 0$. This is again straightforward to integrate with an initial value problem solver. We ultimately seek

$$\frac{\partial \mathcal{Y}_i}{\partial \mu} = Y_{i,\mu}(t_f; \mu, y_0) + F_i(\mathcal{Y}(\mu, y_0); \mu) \frac{\partial t_f}{\partial \mu}.$$

Letting $g_\mu = \partial g / \partial \mu |_{(\mathcal{Y}(\mu, y_0); \mu)}$, again apply the chain rule to find

$$0 = \frac{\partial g(Y(t_f(\mu, y_0); \mu, y_0))}{\partial \mu} = n_k F_k(\mathcal{Y}(\mu, y_0); \mu) \frac{\partial t_f}{\partial \mu} + n_l Y_{l,\mu}(t_f; \mu, y_0) + g_\mu(\mathcal{Y}(\mu, y_0), \mu)$$

or

$$\frac{\partial t_f}{\partial \mu} = -\frac{n_l Y_{l,\mu}(t_f; \mu, y_0)}{n_k F_k(\mathcal{Y}(\mu, y_0); \mu)} - \frac{g_\mu(\mathcal{Y}(\mu, y_0), \mu)}{n_k F_k(\mathcal{Y}(\mu, y_0); \mu)}.$$

Again dropping the arguments of the various functions,

$$\frac{\partial \mathcal{Y}_i}{\partial \mu} = \left(\delta_{il} - \frac{F_i n_l}{n_k F_k} \right) Y_{l,\mu} - \frac{F_i g_\mu}{n_k F_k},$$

with all quantities on the right-hand side again evaluated at $t = t_f(\mu, y_0)$, $y = Y(t_f(\mu, y_0); \mu, y_0) = \mathcal{Y}(\mu, y_0)$.

In the main paper, we also compute the boundary of the region in parameter space in which N becomes negative during the oscillation. This corresponds to solving for a parameter value μ and the corresponding y_0 for which one component of y_0 is equal to zero, and it is straightforward to adapt the methodology above to that case.

4 An asymptotic analysis of limit cycles

Here, we provide an asymptotic description of limit cycles that occur when water input q_{in} as well as cavity opening rates v_o are small. This is the classical case of a glacier-dammed lake in which the filling portion of the jökulhlaup cycle is much slower than the draining portion, and in which the opening of the channel that forms during the jökulhlaup is eventually controlled entirely by wall melting.

The limit cycles we describe allow us to illustrate the key role played by the cavity opening term in allowing a periodic solution without the need to appeal to a moving flow divide in a conduit held open at all times by dissipative melting as in (Fowler, 1999). We do so by dividing the cycle into a number of distinct stages, in each of which only a reduced set of physical processes dominate. In addition, we are able to derive a number of semi-analytical results in the chosen parameter limit: for instance, we can demonstrate that the limit cycle will lead to negative effective pressures at a critical water input rate. This extends the analytical confirmation of limit cycle behaviour beyond the local behaviour near supercritical Hopf bifurcations. Technically, the limit cycles bear close resemblance to some aspects classical relaxation oscillations (Holmes, 1995), but with some key differences (in technical terms, we will see that there is only one ‘slow branch’, with a single ‘fast branch’ connecting a turning point on the slow variable nullcline with another point on the same nullcline).

We consider the model (8) with constitutive relations (3) and $S_0 = \infty$, $V_p = \text{constant}$. This can be rendered in an alternative dimensionless form by defining new scales for S , N and t through $[S]'/[t]' = c_1 c_3 [S]'^\alpha \Psi_0^{3/2} = c_2 [S]' [N]'^n$ and $V_p [N]'/[t]' = c_1 [S]'^\alpha \Psi_0^{1/2}$ and defining corresponding dimensionless variables $S = [S]' S^{**}$, $N = [N]' N^{**}$ and $t = [t]' t^{**}$. The new choice of dimensionless variables yields on substituting and immediately dropping the asterisks again,

$$\dot{S} = S^\alpha |1 - \nu N|^{3/2} + \delta - S |N|^{n-1} N \quad (51a)$$

$$\dot{N} = -\epsilon + S^\alpha |1 - \nu N|^{-1/2} (1 - \nu N) \quad (51b)$$

where $\nu = [N]' / (\Psi_0 L)$, $\delta = u_b h_r / (c_2 [S]' [N]'^n)$ and $\epsilon = q_{in} / (c_1 [S]'^\alpha \Psi_0^{1/2})$.

Note that the new (primed) scales differ from those defined previously in section 2.2, and the dimensionless variables can be related to each other as

$$S^* = V_p^{*n/(n+1-\alpha)} S^{**}, \quad N^* = V_p^{*(\alpha-1)/(n+1-\alpha)} N^{**}, \quad t^* = V_p^{*-n(\alpha-1)/(n+1-\alpha)} t^{**}, \quad (52)$$

while the new dimensionless parameters are related to the old through

$$\epsilon = q_{in}^* V_p^{*- \alpha n / (n+1-\alpha)}, \quad \delta = V_p^{*- \alpha n / (n+1-\alpha)}, \quad \nu = V_p^{*(\alpha-1)/(n+1-\alpha)} / L^*. \quad (53)$$

The new choice of non-dimensionanlization is better suited to exploring the simultaneous limit of small δ and ϵ , while the original choice of scales in section 2.2 was in large part chosen to motivate the choice of V_p , q_{in} and L as the primary controlling variables, and because it makes the relationship with the onset of channelization easier to see, by balancing all four terms in the evolution equation for S .

We assume that the scaled opening and water supply rates are small, so

$$\delta \ll 1, \quad \epsilon \ll 1, \quad (54)$$

as this allows us to apply the method of matched asymptotic expansions. Note that this is equivalent to $V_p^* \gg 1$ (to ensure a small cavity opening rate $\delta \ll 1$) and $q_{in} \ll V_p^{*\alpha n / (n+1-\alpha)}$ (to ensure small ϵ). We also assume that the flow is not dominated by pressure gradients $-\nu N$, as this would require negative N to generate a positive discharge. In other words, we restrict ourselves to $\nu \lesssim 1$. In order to obtain good agreement with the full model of section 2.1, we may expect that pressure gradients need to be small throughout the cycle, so that the crude representation of actual pressure gradients (which would here be $\nu \partial N / \partial x$) by divided differences $-\nu N$ does not affect model results. As we will show, this turns out simply to require $\nu \ll 1$. With large V_p^* , this is more restrictive than merely putting $L^* \gg 1$, but implies

$$L^* \gg V_p^{*(\alpha-1)/(n+1-\alpha)} : \quad (55)$$

For a fixed system size L^* , we expect the lumped model to break down as storage capacity is increased.

In typical drainage models, $\alpha = 4/3$ or $5/4$ while $n = 3$. Below, we will assume that

$$n + 1 > \alpha > 1, \quad (56a)$$

which affects the behaviour of flood initiation, as we shall see. With this constraint, we also have

$$\frac{(\alpha - 1)(n + 1)}{\alpha n} < 1. \quad (56b)$$

It turns out that we need to refine (54): in order for the the steady state solution to (51) not to be stable and there to be no periodic orbits, we need to have

$$\delta \lesssim \epsilon \ll 1; \quad (56c)$$

translated to the original scaling of section 2.2, $\epsilon/\delta = q_{in}^* \sim O(1)$, while the condition for ‘channel-like’ behaviour of the steady state conduit (and hence for instability, see section 3) in the limit of large L^* is $q_{in}^* > 1/(\alpha - 1)$. In addition, we require the constraint

$$\epsilon \lesssim \delta^{(\alpha-1)(n+1)/(\alpha n)}. \quad (56d)$$

We will show that, if the latter constraint is not satisfied, then the re-opening of conduits by dissipation at the beginning of the flood is too slow to prevent water storage from being ‘overfilled’, meaning that sustained negative effective pressures are attained before the flood proper begins. Note that the two constraints (56c) and (56d) are mutually consistent without implying each other: with $\delta \ll 1$ and (56b), $\delta \ll \delta^{(\alpha-1)(n+1)/(\alpha n)}$, so there is a range of values that ϵ can occupy.

We expect a jökulhlaup cycle to consist ostensibly of two parts: a flood component during which there is significant discharge but little recharge of stored water volume, and a post-flood recharge phase during which the conduit has shut down and there is recharge over a much longer time scale, but relatively little discharge. We show below that flood can be identified as an ‘interior layer’ (similar to a boundary layer) in time during which conduit size changes rapidly, with the recharge phase being an ‘outer’ solution in which the conduit is cavity-like with only slow changes in conduit size, and the dynamics of the system is driven entirely by the refilling rate ϵ . We show that in addition, there is a third component in the cycle that we term the ‘flood initiation’, during which dissipation starts to play a significant role in controlling conduit size, but the refilling rate is still significant; in the language of asymptotics, this phase consists of a sequence of nested corner and interior layers. We show that each of those three components of the cycle admits a unique solution that matches asymptotically with the other components to form a limit cycle.

4.1 The flood phase

The scaling in (51) is appropriate during the flood phase of the jökulhlaup cycle, when a initial growth in S driven by the dissipation term $S^\alpha |1 - \nu N|^{3/2}$ is eventually terminated because discharge through the channel increases the effective pressure and therefore both, reduces the dissipation rate and increases the closure rate. The appropriately reduced model for the flood phase is

$$\dot{S} = S^\alpha |1 - \nu N|^{3/2} - S |N|^{n-1} N \quad (57a)$$

$$\dot{N} = S^\alpha |1 - \nu N|^{-1/2} (1 - \nu N) \quad (57b)$$

Since $\alpha > 1$, it is straightforward to see that the large time behaviour of these equations is that N tends to some finite limit N_f , while S tends to zero exponentially as $\exp(-N_f^n t)$, with (57) behaving as $\dot{S} \sim -S|N|^{n-1}N$, $\dot{N} \sim 0$. The final value of N_f is dictated by the initial conditions, which are

$$\tilde{N} \sim \tilde{S} \sim [(\alpha - 1)(-t)]^{-1/(\alpha-1)}. \quad (57c)$$

We will finally be able to justify these in section 4.4, once we have described the recharge and flood initiation phases of the jökulhlaup cycle.

Importantly, the problem (57) contains no parameters, and hence N_f is independent of the exact parameter regime we choose provided the constraints identified above are satisfied. In practice, N_f is obtained by integrating (57) numerically; for the parameter values used in our numerical calculations, $\alpha = 5/4$ and $n = 3$, we obtain with $\nu = 0$

$$N_f = 1.44. \quad (58)$$

As we will see shortly (section 4.2), our asymptotic expansions predict that the recurrence intervals of floods is simply N_f/ϵ at leading order. In practice, this is not particularly well satisfied even for fairly extreme numerical values of δ and ϵ . As we will see in section 4.4, the separation of scales that underlies (57c) relies on $\delta^{-(\alpha-1)/(\alpha n)} \ll 1$. While this is formally true whenever $\delta \ll 1$, note that with the values of $n = 3$ and $\alpha = 5/4$ used in our numerical computations, the exponent on δ becomes very small, $(\alpha - 1)/(\alpha n) = 1/15$.

4.2 The recharge phase

We expect an $O(1)$ effective pressure at the end of the flood, but conduit size S to have become small enough that the cavity opening term in (51) must become important. Evolution of the channel should then also occur on a much longer time scale associated with the recharge rate ϵ . The obvious rescaling to describe the post-flood part of the cycle is therefore

$$\tilde{N} = N, \quad \tilde{S} = \delta^{-1}S, \quad \tilde{t} = \epsilon(t - t_f).$$

where t_f is the time of the last flood. The rescaled equations become

$$\epsilon \frac{d\tilde{S}}{d\tilde{t}} = \delta^{\alpha-1} \tilde{S}^\alpha |1 - \nu \tilde{N}|^{3/2} + 1 - \tilde{S} |\tilde{N}|^{n-1} \tilde{N}, \quad (59a)$$

$$\frac{d\tilde{N}}{d\tilde{t}} = -1 + \delta^\alpha \epsilon^{-1} \tilde{S}^\alpha |1 - \nu \tilde{N}|^{-1/2} (1 - \nu \tilde{N}). \quad (59b)$$

Given $\delta^\alpha \ll \delta \lesssim \epsilon$, this can be reduced to $\tilde{S} = \tilde{N}^{-n}$ and

$$\frac{d\tilde{N}}{d\tilde{t}} = -1 \quad (60)$$

Matching with the flood solution gives $\tilde{N}(0) = N_f$ at the beginning of the recharge phase, and we have

$$\tilde{N} = N_f - \tilde{t}. \quad (61)$$

At late stages $\tilde{t} \sim N_f$ in the recharge phase, effective pressure approaches zero and conduit size \tilde{S} becomes large. A further rescaling is required here, and we see that the recharge phase really consists of two distinct parts. At the end of the recharge phase, we expect dissipation in the conduit to reappear at leading order again, as this will be necessary to restart a flood. We term this stage the flood initiation phase. In the language of matched asymptotic expansions, the initiation phase give the flood the structure of a sequence of nested boundary layers, or more specifically, of nested corner and boundary layers.

These additional layers, as well as the main flood phase of section 4.1, all involve faster time scales than that of the main recharge phase. Moreover, the recharge phase lasts until $\tilde{t} \sim N_f$, from which the periodicity of the flood cycle at leading order is $\tilde{t} = N_f$, or equally, $t = N_f/\epsilon$. In dimensional terms,

$$t_{period} = N_f c_1^{\alpha/(n+1-\alpha)} c_2^{-1/(n+1-\alpha)} c_3^{1/(n+1-\alpha)} \Psi_0^{(1+2\alpha)/[2(n+1-\alpha)]} V_p^{n/(n+1-\alpha)} q_{in}^{-1}. \quad (62)$$

4.3 Flood initiation

The relevant rescaling to describe the onset of significant dissipation in the conduit is

$$\hat{N} = \delta^{-(\alpha-1)/(\alpha n)} \tilde{N}, \quad \hat{S} = \delta^{(\alpha-1)/\alpha} \tilde{S}, \quad \hat{t} = \delta^{-(\alpha-1)/(\alpha n)} (\tilde{t} - N_f)$$

and gives

$$\epsilon \delta^{-(\alpha-1)(n+1)/(\alpha n)} \frac{d\hat{S}}{d\hat{t}} = \hat{S}^\alpha |1 - \nu \delta^{(\alpha-1)/(\alpha n)} \hat{N}|^{3/2} + 1 - \hat{S} |\hat{N}|^{n-1} \hat{N}, \quad (63a)$$

$$\frac{d\hat{N}}{d\hat{t}} = -1 + \delta \epsilon^{-1} \hat{S}^\alpha |1 - \nu \delta^{(\alpha-1)/(\alpha n)} \hat{N}|^{1/2} (1 - \nu \delta^{(\alpha-1)/(\alpha n)} \hat{N}). \quad (63b)$$

With the constraints (54), (56c), we can reduce this to

$$\epsilon \delta^{-(\alpha-1)(n+1)/(\alpha n)} \frac{d\hat{S}}{d\hat{t}} = \hat{S}^\alpha + 1 - \hat{S} |\hat{N}|^{n-1} \hat{N}, \quad (64a)$$

$$\frac{d\hat{N}}{d\hat{t}} = -1 + \delta \epsilon^{-1} \hat{S}^\alpha. \quad (64b)$$

and matching with the main recharge phase solution $(\tilde{S}, \tilde{N}) = (1/(N_f - t_f)^n, N_f - t_f)$ gives

$$\hat{N} \sim -\hat{t}, \quad \hat{S} \sim 1/|\hat{t}|^n \quad \text{as} \quad \hat{t} \rightarrow -\infty. \quad (65)$$

Now we can see why $\delta \lesssim \epsilon$ is necessary. If the coefficient of the second term on the right-hand side of (64b) were large, we would always be able to find a steady state solution $\hat{S}^\alpha = \epsilon \delta^{-1} \ll 1$, $|\hat{N}|^{n-1} \hat{N} = \hat{S}/(1 + \hat{S}^\alpha) = \epsilon \delta^{-1}/(1 + \epsilon \delta^{-1}) \sim \epsilon \delta^{-1}$, and it is straightforward to show that this steady state is stable. The system could therefore settle into this steady state and no further floods would need to occur. We return to this scenario in section 4.5, where we state a precise lower bound on $\delta \epsilon^{-1}$ required for the steady state not to be attained.

There are now two versions of the model that could apply, depending on whether $\epsilon\delta^{-(\alpha-1)(n+1)/(\alpha n)}$ is small or not. The former physically corresponds to the conduit remaining in a pseudo-steady state, with drainage of the reservoir starting to affect the evolution of N through the outflow term $S^\alpha|1 - \nu N|^{-1/2}(1 - \nu N)$ in (51). The latter by contrast allows a lag between effective pressure changes and the evolution of S , so that the time derivative \dot{S} in (51) potentially features at leading order, while the lake has not yet begun to drain effectively and the outflow term remains small in the evolution equation for N .

Consider first the second of these two cases: suppose that $\epsilon\delta^{-(\alpha-1)(n+1)/(\alpha n)} \sim 1$. The case $\epsilon\delta^{-(\alpha-1)(n+1)/(\alpha n)} \ll 1$ will be described in section 4.5. Recall from (56a) that $n \geq \alpha - 1$, in line with typical assumptions in glaciology. In that case $\epsilon\delta^{-(\alpha-1)(n+1)/(\alpha n)} \gtrsim 1$ implies

$$\delta\epsilon^{-1} \lesssim \delta^{(n+1-\alpha)/(\alpha n)} \ll 1,$$

and we are reduced to

$$\epsilon\delta^{-(\alpha-1)(n+1)/(\alpha n)} \frac{d\hat{S}}{d\hat{t}} = \hat{S}^\alpha + 1 - \hat{S}|\hat{N}|^{n-1}\hat{N}, \quad (66a)$$

$$\frac{d\hat{N}}{d\hat{t}} = -1, \quad (66b)$$

Here we can see why we imposed the constraint (56d). If instead we had $\epsilon\delta^{-(\alpha-1)(n+1)/(\alpha n)} \gg 1$, then (66) would further reduce to $d\hat{S}/d\hat{t} = 0$, and there would be nothing to prevent \hat{N} from becoming large and negative. In fact, a further rescaling would become necessary to capture the initiation of the next flood, which is necessary to allow N to increase again. Assuming that sustained negative effective pressures are not realistic and that additional physics is required in that case (Hewitt and others, 2012), we insist instead on the constraint (56d).

If therefore $\epsilon\delta^{-(\alpha-1)(n+1)/(\alpha n)} = O(1)$, we instead expect a solution that has $\hat{N} = -\hat{t}$, with \hat{S} satisfying

$$\epsilon\delta^{-(\alpha-1)(n+1)/(\alpha n)} \frac{d\hat{S}}{d\hat{t}} = \hat{S}^\alpha + 1 + \hat{S}|\hat{t}|^{n-1}\hat{t} \quad (67)$$

At late times, the right-hand side is dominated by the \hat{S}^α term, and the solution will experience finite-time blow-up as \hat{t} approaches some limit $\hat{t} \rightarrow \hat{t}_i$, where

$$\hat{S} \sim \frac{\epsilon^{1/(\alpha-1)}\delta^{-(n+1)/(\alpha n)}}{[(\alpha-1)(\hat{t}_i - \hat{t})]^{1/(\alpha-1)}}, \quad \hat{N} \sim -\hat{t}_i. \quad (68)$$

With the initial conditions given by (65), the time \hat{t}_i depends purely on the remaining model parameter $\epsilon\delta^{-(\alpha-1)(n+1)/(\alpha n)}$, and therefore so does the final value of \hat{N} . The relationship between

$$\hat{N}_c = -\hat{t}_i$$

and $\epsilon\delta^{-(\alpha-1)(n+1)/(\alpha n)}$ can be computed numerically by integrating the system (66) and is shown in figure 1 for $n = 3$ and $\alpha = 5/4$. As we expect, growth of the solution \hat{S}

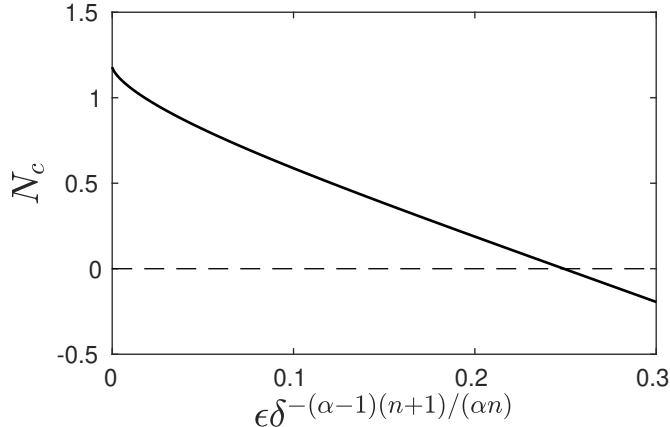


Figure 1: The finite-time blow-up value \hat{N}_c plotted against $\epsilon\delta^{-(\alpha-1)(n+1)/(\alpha n)}$ for $\alpha = 5/4$ and $n = 3$.

takes a longer time for larger $\epsilon\delta^{-(\alpha-1)(n+1)/(\alpha n)}$, leading to progressively more negative \hat{N}_c .

Importantly, there is a critical value γ_c of $\epsilon\delta^{-(\alpha-1)(n+1)/(\alpha n)}$ when we first see \hat{N}_c become negative; as we will see below, \hat{N}_c is the smallest effective pressure during the flood cycle, so this threshold corresponds to the parameter regime in which negative effective pressures first appear. For the parameter values $\alpha = 5/4$ and $n = 3$,

$$\gamma_c = 0.25.$$

In terms of the original, unscaled parameters, the threshold for negative effective pressures is at leading order

$$q_{in} = \gamma_c c_1^{(n+1)/(\alpha n)} c_2^{-1/n} c_3^{(n+1)/(\alpha n)} \Psi_0^{3(n+1)/(2\alpha n)} (u_b h_r)^{-(\alpha-1)(n+1)/(\alpha n)} V_p, \quad (69)$$

with smaller values of q_{in} maintaining positive effective pressures throughout the limit cycle. As we show in the main text, this generally underestimates the value of q_{in} at which effective pressures first appear.

To see that $\hat{N}_c = -\hat{t}_i$ is the minimum effective pressure in the flood cycle, and to complete the description of the cycle, we have to recognize that finite-time blow-up actually corresponds to \hat{S} becoming large as part of the runaway growth of the channel at the start of the next flood. Channel size does not actually become infinite: the next flood itself must instead be described by a further rescaling that captures again the draining of stored water, which allows effective pressure to increase again and stops channel size from becoming infinite. This leads us back to the flood phase described in section 4.1.

4.4 Flood initial conditions and uniqueness of the flood solution

The rescaling mentioned above must ultimately recover the original variables (S, N) . However, proper matching of effective pressure changes requires that we do not go

immediately to the full flood phase variables, but introduce a further two layers in which conduit size already undergoes runaway growth while effective pressure is beginning to be affected by drainage through the rapidly opening channel.

The first of these is a corner layer in which the (S, N) orbit crosses the N -nullcline, allowing effective pressure to start increasing again. Put

$$\check{S} = (\delta\epsilon^{-1})\hat{S}, \quad \check{N} = \hat{N}, \quad \check{\mathcal{T}} = \delta^{(\alpha-1)/(\alpha n)}\epsilon^{-1/\alpha}(\hat{t} - \hat{t}_i). \quad (70)$$

Note that

$$\epsilon^{-1/\alpha}\delta^{(\alpha-1)/(\alpha n)} = (\epsilon\delta^{-(\alpha-1)(n+1)/(\alpha n)})^{-1/\alpha}\delta^{-(\alpha-1)(n+1-\alpha)/(\alpha^2 n)},$$

which is large in the parameter regime under consideration, so $\check{\mathcal{T}}$ is a fast time scale compared with \hat{t} . We obtain

$$\frac{d\check{S}}{d\check{\mathcal{T}}} = \check{S}^\alpha \left| 1 - \nu\delta^{(\alpha-1)/(\alpha n)}\hat{N} \right|^{3/2} + \delta\epsilon^{-1} \left(1 - \check{S}|\check{N}|^{n-1}\check{N} \right); \quad (71a)$$

$$\epsilon^{-1/\alpha}\delta^{(\alpha-1)/(\alpha n)}\frac{d\check{N}}{d\check{\mathcal{T}}} = -1 + \check{S}^\alpha \left| 1 - \nu\delta^{(\alpha-1)/(\alpha n)}\hat{N} \right|^{1/2} \left(1 - \nu\delta^{(\alpha-1)/(\alpha n)}\hat{N} \right) \quad (71b)$$

subject to matching with the solution (66), so

$$\check{S} \sim [(\alpha-1)(-\check{\mathcal{T}})]^{-1/(\alpha-1)}, \quad \check{N} \sim \hat{N}_c - \epsilon^{-1/\alpha}\delta^{-(\alpha-1)/(\alpha n)}\check{\mathcal{T}} \quad (72)$$

as $\check{\mathcal{T}} \rightarrow -\infty$. We expand

$$\check{N} \sim \hat{N}_c + \epsilon^{1/\alpha}\delta^{-(\alpha-1)/(\alpha n)}\check{N}_1. \quad (73)$$

With this expansion, we obtain

$$\frac{d\check{S}}{d\check{\mathcal{T}}} = \check{S}^\alpha, \quad (74a)$$

$$\frac{d\check{N}_1}{d\check{\mathcal{T}}} = -1 + \check{S}^\alpha \quad (74b)$$

with solution

$$\check{S} \sim [(\alpha-1)(-\check{\mathcal{T}})]^{-1/(\alpha-1)}, \quad \check{N}_1 = -\check{\mathcal{T}} + [(\alpha-1)(-\check{\mathcal{T}})]^{-1/(\alpha-1)}. \quad (75)$$

The corner layer describes the change in sign of $d\check{N}/d\check{\mathcal{T}}$ that happens as the orbit crosses the nullcline; this is the lake highstand. While this corresponds to an $O(1)$ change in the derivative, it involves only a higher order change in \check{N} itself. To describe the increase in effective pressure itself, we require a further rescaling of the time variable

$$\begin{aligned} \check{S} &= \check{S} = (\delta\epsilon^{-1})\hat{S}, & \check{N} &= \check{N} = \hat{N}, \\ \check{\mathcal{T}} &= \delta^{-(\alpha n+1)(\alpha-1)/(\alpha n)}\epsilon^{(\alpha-1)+1/\alpha}\check{\mathcal{T}} = (\delta\epsilon^{-1})^{-(\alpha-1)}(\hat{t} - \hat{t}_i). \end{aligned} \quad (76)$$

Note that

$$\delta^{-(\alpha n+1)(\alpha-1)/(\alpha n)} \epsilon^{(\alpha-1)+1/\alpha} = \epsilon \delta^{-(n+1)(\alpha-1)/(\alpha n)} (\epsilon \delta^{-1})^{(\alpha-1)^2/\alpha}$$

and this is large under the assumed parameter regime, so \check{t} is fast compared with $\check{\mathcal{T}}$. From (63) and using the constraints (56), this yields at leading order

$$\epsilon \delta^{-(\alpha-1)(n+1)/(\alpha n)} \frac{d\check{S}}{d\check{t}} = \check{S}^\alpha, \quad (77a)$$

$$\frac{d\check{N}}{d\check{t}} = \check{S}^\alpha \quad (77b)$$

with matching conditions with (68) being

$$\check{S} \sim \frac{\epsilon^{1/(\alpha-1)} \delta^{-(n+1)/(\alpha n)}}{[(\alpha-1)(-\check{t})]^{1/(\alpha-1)}}, \quad \check{N} \sim \hat{N}_c \quad (78)$$

The solution for \check{S} remains simply equal to $\epsilon^{1/(\alpha-1)} \delta^{-(n+1)/(\alpha n)} / [(\alpha-1)(-\check{t})]^{1/(\alpha-1)}$, while $\check{N} = \epsilon \delta^{-(\alpha-1)(n+1)/(\alpha n)} \check{S} - \hat{t}_i$. We still have finite time blow-up at $\check{t} = 0$, with behaviour as $\check{t} \rightarrow 0^-$ of

$$\check{S} \sim \frac{\epsilon^{1/(\alpha-1)} \delta^{-(n+1)/(\alpha n)}}{[(\alpha-1)(-\check{t})]^{1/(\alpha-1)}}, \quad \check{N} \sim \epsilon \delta^{-(\alpha-1)(n+1)/(\alpha n)} \check{S} \quad (79)$$

Finally, to describe the full flood including termination, we need to return to the original scaled variables. The relevant rescaling is

$$S = \epsilon \delta^{-(\alpha-1)/\alpha} \check{S}, \quad N = \delta^{(\alpha-1)/(\alpha n)} \check{N}, \quad t = \epsilon^{-\alpha} \delta^{(\alpha-1)(1+\alpha n)/(\alpha n)} \check{t}. \quad (80)$$

This retrieves the original version of the model (51) and hence the leading order flood-stage version (57). Matching with the solution (79) corresponds to

$$N \sim S \sim [(\alpha-1)(-t)]^{-1/(\alpha-1)} \quad \text{as} \quad t \rightarrow -\infty. \quad (81)$$

This is the set of initial conditions that formally must be satisfied by the solution to (57) and, as discussed, then provides the end-of-flood effective pressure N_f . Note however that asymptotic matching here makes use of $\delta^{(\alpha-1)/(\alpha n)} \ll 1$ when matching N and \check{N} , meaning $N \rightarrow 0$ as $t \rightarrow -\infty$. As discussed in section 4.1, in practice the exponent $(\alpha-1)/(\alpha n)$ is small, and the separation of scales is weak.

Persisting with the formal asymptotic result, N_f is the only parameter in the recharge phase solution (61), and dictates the repeat period. In other words, if matching with (79) defines a unique solution to the flood problem (57), our asymptotic limit cycle solution is complete as both, the flood and the recharge phase solutions are then unique.

Therefore the only important quality we still need to establish is therefore that the set of initial conditions (81) defines a unique solution to (57) and hence a unique final effective pressure N_f . Let $P = N/S$, and switch to (S, P) as dependent variables.

From (81), we see that $S \rightarrow 0$ while $P \sim 1$ remains bounded as $t \rightarrow -\infty$; the impotence of introducing the corner layer (77) is that it permits us to say not only that $N \rightarrow 0$ for $t \rightarrow -\infty$ (as we could have gleaned from (68)), but that N/S cannot diverge either. This change of variables turns (57) into

$$\dot{S} = S^{\alpha-1} [S|1 - \nu SP|^{3/2} - S^{n+2-\alpha}|P|^{n-1}P] \quad (82a)$$

$$\dot{P} = S^{\alpha-1} [1 - \nu SP|^{-1/2}(1 - \nu SP) - |1 - \nu SP|^{3/2}P + S^{n+1-\alpha}|P|^{n+1}] \quad (82b)$$

The solution must now approach the fixed point of the system (82) at $(S, P) = (0, 1)$ (note that to identify this as a fixed point, we require again the constraint (56a)). We therefore need to determine whether orbits that approach this fixed point as $\zeta \rightarrow -\infty$ are unique. The prefactor $S^{\alpha-1}$ can be absorbed into a new-time like variable ζ by defining

$$\frac{dt}{d\zeta} = S^{-(\alpha-1)}, \quad (83)$$

which leads to

$$\frac{dS}{d\zeta} = S|1 - \nu SP|^{3/2} - S^{n+2-\alpha}|P|^{n-1}P \quad (84a)$$

$$\frac{dP}{d\zeta} = |1 - \nu SP|^{-1/2}(1 - \nu SP) - |1 - \nu SP|^{3/2}P + S^{n+1-\alpha}|P|^{n+1} \quad (84b)$$

It is straightforward to show by linearizing about this fixed point as $S = S', P = 1 + P'$ that it is a saddle point with

$$S'_\zeta \sim S', \quad P'_\zeta \sim -P'.$$

The unstable manifold of this saddle point is therefore a unique orbit that approaches this fixed point as $\zeta \rightarrow -\infty$ (Wiggins, 2003).

From the above, we also get $S \sim \exp(\zeta)$ as $\zeta \rightarrow -\infty$. It can then be confirmed that the limit $\zeta \rightarrow -\infty$ does correspond $t \rightarrow -\infty$ (rather than t reaching a finite limit), with S behaving as $S \sim [-\alpha(t - t_0)]^{-1/(\alpha-1)}$ for some t_0 . To match successfully as required by (81), we require $t_0 = 0$, and this fixes the time origin along the unique orbit that connects into the fixed point $(S, P) = (0, 1)$, and we obtain a unique flood solution.

4.5 The initiation phase revisited

We pursued the flood initiation problem in section 4.3 in the limit $\epsilon\delta^{-(\alpha-1)(n+1)/(\alpha n)} = O(1)$. We can also do the same for $\epsilon\delta^{-(\alpha-1)(n+1)/(\alpha n)} \ll 1$ but allow $\delta\epsilon^{-1} = O(1)$ in (64). The flood initiation phase then becomes even more complicated (with no fewer than three nested corner and boundary layers) but still leads to the same matching conditions (81) at the beginning of the flood phase, and a unique asymptotic limit cycle solution.

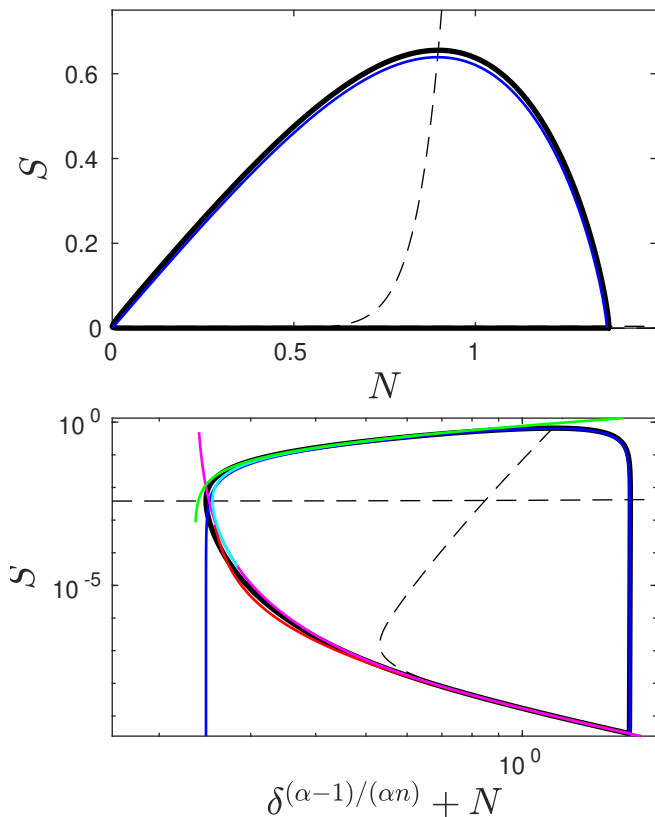


Figure 2: Phase plane solution for the full system (51) (black) plotted against the asymptotic solution (coloured lines, $\epsilon = 9.60 \times 10^{-4}$, $\delta = 7.33 \times 10^{-10}$, $\nu = 0.156$, $\alpha = 5/4$, $n = 3$). Top bottom panel shows the same results as the top, but adopts logarithmic horizontal scale with an offset of 0.246 to avoid negative values of the abscissa. Dashed lines show the nullclines. Blue is the flood phase solution (57), magenta the recharge phase (59), red the flood initiation phase (66), light blue the corner layer (74) and green the early channel growth phase (77).

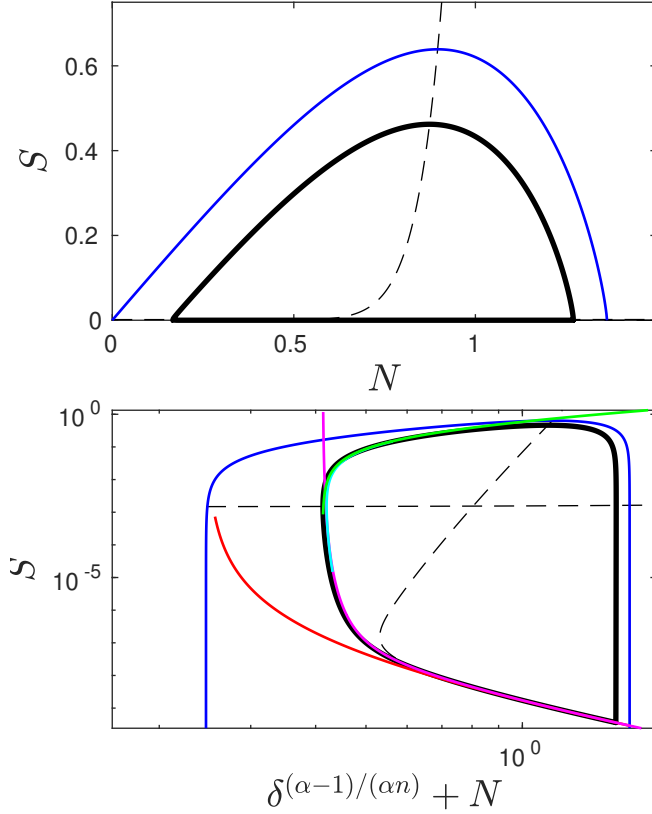


Figure 3: Phase plane solution for the full system (51) (black) plotted against the asymptotic solution (coloured lines, $\epsilon = 2.92 \times 10^{-4}$, $\delta = 7.33 \times 10^{-10}$, $\nu = 0.156$). Same plotting scheme as figure 2, but without the horizontal offset in the bottom panel. Note that all asymptotic solutions but the flood phase agree well with the solution of the full model in the region where they are valid; this is because the flood phase formally satisfies the boundary conditions $(N, S) \rightarrow (0, 0)$ as $t \rightarrow -\infty$, but the order of the omitted term is $\delta^{(\alpha-1)/(\alpha n)} \sim 0.246$ despite having $\delta \sim 10^{-10}$. The reason for the apparently good agreement in figure 2 is in fact that the solution shown there corresponds to $\tilde{N}_c = 0$, so that $N = 0$ at the beginning of the flood phase is a good approximation.

We only sketch this very briefly here. At leading order, (64) becomes

$$0 = \hat{S}^\alpha + 1 - \hat{S}|\hat{N}|^{n-1}\hat{N}, \quad (85a)$$

$$\frac{d\hat{N}}{d\hat{t}} = -1 + \delta\epsilon^{-1}\hat{S}^\alpha. \quad (85b)$$

(85a) defines \hat{S} implicitly as a function of \hat{N} . Where it exists, this function has two branches. We must pick the cavity-like branch on which \hat{S} is a decreasing function of \hat{N} to match with the recharge phase solution through (65). This is also required in order to obtain a stable solution that justifies the neglect of the time-derivative on the right-hand side of (64a). (85b) then takes the form of a first-order ordinary differential equation in \hat{N} , and this will evolve towards a stable steady state with $\hat{S}^\alpha = \epsilon\delta^{-1}$ if the latter exists.

Such a steady state would prevent repeated floods. The steady state need not exist, however, as there need not be a value of \hat{N} for which $\hat{S}^\alpha = \epsilon\delta^{-1}$ with \hat{S} on the cavity-like solution branch. The solution to (85a) ceases to exist when the minimum with respect to \hat{S} of the right-hand side of (85a) is positive, which occurs when $\hat{N}^n > \hat{N}_c^n := \alpha/(\alpha-1)^{(\alpha-1)/\alpha}$. Cavity-like solutions for \hat{S} are all smaller than the critical value $\hat{S}_c := (\alpha-1)^{-1/\alpha}$ attained at $\hat{N} = \hat{N}_c$. Repeated floods therefore occur if

$$\hat{S}_c^\alpha = 1/(\alpha-1) < \epsilon\delta^{-1}. \quad (86)$$

We will assume this to be the case.

As the (saddle-node) bifurcation point in (85a) is approached, we have to switch to a faster time scale to capture the rapid enlargement of the conduit through wall melting that occurs once \hat{N} drops low enough. Let \hat{t}_c be the time at which the reduced system (85) would attain $(\hat{S}, \hat{N}) = (\hat{S}_c, \hat{N}_c)$. The relevant rescaling to capture the first stage in that enlargement, when ongoing reduction in effective pressure is an important factor in starting the process, is

$$\begin{aligned} \check{S} &= \epsilon^{-1/3}\delta^{(\alpha-1)(n+1)/(3\alpha n)}(\hat{S} - \hat{S}_c), & \check{N} &= \epsilon^{-2/3}\delta^{2(\alpha-1)(n+1)/(3\alpha n)}(\hat{N} - \hat{N}_c), \\ \check{t} &= \epsilon^{-2/3}\delta^{2(\alpha-1)(n+1)/(3\alpha n)}(\hat{t} - \hat{t}_c). \end{aligned} \quad (87)$$

At leading order, the problem (63) becomes under this rescaling

$$\frac{d\check{S}}{d\check{t}} = \alpha(\alpha-1)\hat{S}_c^{\alpha-2}\check{S}^2 - n\hat{S}_c|\hat{N}_c|^{n-1}\check{N} \quad (88a)$$

$$\frac{d\check{N}}{d\check{t}} = -1 + \delta\epsilon^{-1}\hat{S}_c^\alpha \quad (88b)$$

with matching conditions as $\check{t} \rightarrow -\infty$ being $\check{S} \sim [n\alpha^{-1}(\alpha-1)^{-1}\hat{S}_c^{3-\alpha}|\hat{N}_c|^{n-1}]^{1/2}\check{N}^{1/2}$ where $\check{N} \sim -\left(1 - \delta\epsilon^{-1}\hat{S}_c^\alpha\right)\check{t}$

With (86), it is clear that \check{N} simply decreases linearly on this timescale, and that the quadratic term in \check{S} in (88a) will eventually dominate, leading once more to a solution with finite-time blow-up, this time behaving as

$$\check{S} \sim [\alpha(\alpha-1)(\check{t}_b - \check{t})]^{-1}. \quad (89)$$

Of course, this again means simply that we need a further rescaling as the blow-up time \check{t}_b is approached. Note that \check{S} represents a perturbation around the critical conduit size \hat{S}_c ; the rescaling must represent $O(1)$ changes in S due to dissipation in the conduit, but happening on a faster time scale than \check{t} . The relevant rescaling is

$$\acute{S} = \hat{S}, \quad \acute{N} = \hat{N}, \quad \acute{t} = \epsilon^{-1/3} \delta^{(\alpha-1)(n+1)/(3\alpha n)} (\check{t} - \check{t}_b)$$

which leads to, at leading order,

$$\frac{d\acute{S}}{d\acute{t}} = \acute{S}^\alpha + 1 - \acute{S}|\acute{N}|^{n-1}\acute{N}, \quad (90a)$$

$$\frac{d\acute{N}}{d\acute{t}} = 0. \quad (90b)$$

Matching with the solution of (88) gives $\acute{S} \sim \hat{S}_c + [\alpha(\alpha-1)(-\acute{t})]^{-1}$, $\acute{N} \sim \hat{N}_c$ as $\acute{t} \rightarrow -\infty$. Hence $\acute{N} = \hat{N}_c$ throughout, and the layer (88) simply describes the initial growth of the solution of the system (90) away from its fixed point $(\acute{S}, \acute{N}) = (\hat{S}_c, \hat{N}_c)$. Note that the orbit crosses the nullcline in this layer, which occurs (a higher order correction to $d\acute{N}/d\acute{t}$) when $\acute{S}^\alpha = \epsilon \delta^{-1} > \hat{S}_c^\alpha$.

\acute{S} still exhibits finite time blow-up, this time as $\acute{S} \sim [(\alpha-1)(-\acute{t})]^{1/(\alpha-1)}$. We formally need an initial growth layer analogous to (77), in which effective pressure actual starts to grow as a result of drainage through the growing channel, to match fully with the flood solution in section 4.1 as was done in section 4.4 for the case $\epsilon \delta^{-(\alpha-1)(n+1)/(\alpha n)} = O(1)$. The last rescaling necessary to make this work is

$$\dot{S} = \delta^{(n+1-\alpha)/(\alpha n)} \acute{S}, \quad \dot{N} = \acute{N}, \quad \dot{t} = \delta^{(n+1-\alpha)(\alpha-1)/(\alpha n)} \acute{t}. \quad (91)$$

At leading order, this yields

$$\frac{d\dot{S}}{d\dot{t}} = \dot{S}^\alpha, \quad (92a)$$

$$\frac{d\dot{N}}{d\dot{t}} = \dot{S}^\alpha. \quad (92b)$$

with matching conditions $\dot{S} \sim [(\alpha-1)(-\dot{t})]^{1/(\alpha-1)}$, $\dot{N} \sim \hat{N}_c$; this initial growth layer has a solution behaving as $\dot{S} \sim [(\alpha-1)(-\dot{t})]^{1/(\alpha-1)}$, $\dot{N} \sim \dot{S}$ as $\dot{t} \rightarrow 0^-$. This leads to the same matching conditions (81) with the flood problem as before, ensuring again a unique flood solution.

5 An unrealistic solution: flood cycles with large water supply

Key to our asymptotic solution in the previous section was the small water supply ϵ , relative to the size of the water reservoir. As discussed, even relatively moderate $\epsilon \sim \delta^{(n+1)(\alpha-1)/(\alpha n)}$ can lead to effective pressures becoming negative, for which the

underlying model is not designed. In this section, we discuss briefly what happens formally in the model if we put $\delta \lesssim 1$ (relaxing the previous requirements) but impose $\epsilon \gg 1$. This is the limit of large water supply rates; in terms of the original scaling of section 2.2, we require

$$q_{in}^* \gg V_p^{*\alpha n/(n+1-\alpha)}.$$

The appropriate rescaling becomes

$$N = \epsilon^{1/(n+1)} \mathcal{N}, \quad S = \epsilon^{1/\alpha} \mathcal{S}, \quad t = \epsilon^{-n/(n+1)} \mathcal{T}. \quad (93)$$

Substituting in (51),

$$\frac{d\mathcal{S}}{d\mathcal{T}} = \epsilon^{-(n+1-\alpha)/[\alpha(n+1)]} \mathcal{S}^\alpha |1 - \nu \epsilon^{1/(n+1)} \mathcal{N}|^{3/2} + \delta \epsilon^{-(\alpha n + n + 1)/[\alpha(n+1)]} - \mathcal{S} |\mathcal{N}|^{n-1} \mathcal{N} \quad (94a)$$

$$\frac{d\mathcal{N}}{d\mathcal{T}} = -1 + \mathcal{S}^\alpha |1 - \nu \epsilon^{1/(n+1)} \mathcal{N}|^{-1/2} (1 - \nu \epsilon^{1/(n+1)} \mathcal{N}) \quad (94b)$$

We expect that the lumped model remains accurate only if the $O(\nu \epsilon^{1/(n+1)})$ pressure gradient terms stay small, which imposes the stronger restriction

$$\nu \ll \epsilon^{-1/(n+1)} \quad (95)$$

or, in terms of the scalings of section 2.2,

$$V_p^* L^* \gg q_{in}^*.$$

This can be compared with the similar restriction (55) of section 4: by contrast with the latter, we now have a better approximation of the pressure gradient for fixed system size L^* if V_p^* is larger. For fixed V_p^* , the approximation eventually breaks down as water supply q_{in}^* is increased.

Suppose that (95) holds to all orders required below. In this case, we can sketch out the relevant solution structure. At leading order,

$$\begin{aligned} \frac{d\mathcal{S}}{d\mathcal{T}} &= -\mathcal{S} |\mathcal{N}|^{n-1} \mathcal{N}, \\ \frac{d\mathcal{N}}{d\mathcal{T}} &= \mathcal{S}^\alpha - 1. \end{aligned}$$

Defining a new variable

$$\zeta = \log(\mathcal{S}), \quad (96)$$

we obtain the Hamiltonian system

$$\frac{d\zeta}{d\mathcal{T}} = -\frac{\partial H}{\partial \mathcal{N}}, \quad (97a)$$

$$\frac{d\mathcal{N}}{d\mathcal{T}} = \frac{\partial H}{\partial \zeta}, \quad (97b)$$

$$H(\zeta, \mathcal{N}) = \frac{1}{n+1} |\mathcal{N}|^{n+1} - \zeta + \alpha^{-1} \exp(\alpha \zeta). \quad (97c)$$

H is convex with isolines that form closed loops; these are the orbits followed by (ζ, \mathcal{N}) at leading order. The problem is not truly Hamiltonian of course; rather, its value $\mathcal{H}(\mathcal{T}) = H(\zeta(\mathcal{T}), \mathcal{N}(\mathcal{T}))$ evolves slowly. Retaining higher order terms except those that are small by (95), multiplying (94a) by $S^{-1}\partial H/\partial\zeta$ yields

$$\frac{\partial H}{\partial\zeta} \frac{d\zeta}{d\mathcal{T}} = -\frac{\partial H}{\partial\mathcal{N}} \frac{\partial H}{\partial\zeta} + \epsilon^{-(n+1-\alpha)/[\alpha(n+1)]} \left\{ \exp[(\alpha-1)\zeta] + \delta\epsilon^{-1} \exp(-\zeta) \right\} \frac{\partial H}{\partial\zeta} \quad (98)$$

while multiplying (94b) by $\partial H/\partial\mathcal{N}$ gives

$$\frac{\partial H}{\partial\mathcal{N}} \frac{d\mathcal{N}}{d\mathcal{T}} = \frac{\partial H}{\partial\zeta} \frac{\partial H}{\partial\mathcal{N}}. \quad (99)$$

Hence, by adding,

$$\frac{\partial \mathcal{H}}{\partial \mathcal{T}} = \epsilon^{-(n+1-\alpha)/[\alpha(n+1)]} \left[\exp[(\alpha-1)\zeta] + \delta\epsilon^{-1} \exp(-\zeta) \right] \frac{\partial H}{\partial \zeta} \quad (100)$$

$$= \epsilon^{-(n+1-\alpha)/[\alpha(n+1)]} \left[\exp[(2\alpha-1)\zeta] - \exp[(\alpha-1)\zeta] + \delta\epsilon^{-1} \left\{ \exp[(\alpha-1)\zeta] - \exp(-\zeta) \right\} \right]. \quad (101)$$

To capture the slow change in H implied by this, we have to go to higher order, defining a slow time variable T through

$$\mathcal{T} = \epsilon^{(n+1-\alpha)/[\alpha(n+1)]} T$$

and expanding

$$\mathcal{H} = H_0 + \epsilon^{(n+1-\alpha)/[\alpha(n+1)]} H_1.$$

We apply a standard multiple scales expansion: we write all dependent variables explicitly as functions of \mathcal{T} and T , and hence replace the ordinary derivative with respect to \mathcal{T} by

$$\frac{d}{d\mathcal{T}} = \frac{\partial}{\partial \mathcal{T}} + \epsilon^{-(n+1-\alpha)/[\alpha(n+1)]} \frac{\partial}{\partial T}$$

Then

$$\frac{\partial H_0}{\partial T} + \frac{\partial H_1}{\partial \mathcal{T}} = \exp[(2\alpha-1)\zeta] - \exp[(\alpha-1)\zeta] + \delta\epsilon^{-1} \left\{ \exp[(\alpha-1)\zeta] - \exp(-\zeta) \right\} \quad (102)$$

Note that the $\delta\epsilon^{-1}$ terms are apparently small; we retain them for reasons that will become apparent shortly.

As is standard in multiple scales problems (Holmes, 1995), we treat T and \mathcal{T} as independent and require that all dependent variables are bounded functions of the inner variable \mathcal{T} . In the present case, we know that they are periodic with the period t_p given by the periodicity of the leading order solution. Defining an averaging operator

$$\langle \cdot \rangle = \frac{1}{t_p} \int_0^{t_p} \cdot d\mathcal{T},$$

we can conclude that

$$\left\langle \frac{dH_1}{d\mathcal{T}} \right\rangle = 0$$

and, with the leading order Hamiltonian H_0 independent of \mathcal{T} ,

$$\frac{dH_0}{dT} = \langle \exp[(2\alpha - 1)\zeta] \rangle - \langle \exp[(\alpha - 1)\zeta] \rangle + \delta\epsilon^{-1} \{ \langle \exp[(\alpha - 1)\zeta] \rangle - \langle \exp(-\zeta) \rangle \}. \quad (103)$$

The point is that the terms on the right-hand side, averaged over a single orbital period as indicated, are functions of H_0 only at leading order: the shape of the orbit is all that matters, and is determined uniquely by the value H_0 of the Hamiltonian and the parameters of the model. We know that $H(\zeta, \mathcal{N}) = H_0$, so implicitly we can find a multivalued function F such that

$$\mathcal{N} = F(H_0, \zeta) = \pm(n+1)^{1/(n+1)} (H_0 + \zeta - \alpha^{-1} \exp(\alpha\zeta))^{1/(n+1)}. \quad (104)$$

Trivially, H is unchanged by changing the sign of \mathcal{N} , and the orbit is symmetric about the \mathcal{N} -axis. Therefore it suffices to take the averaging integrals in (103) over half the orbit and multiply by two, allowing us to pick for instance the ‘+’ sign in ‘ \pm ’ in (104). With that choice, ζ decreases along the relevant half of the orbit from ζ_+ to ζ_- , where both are roots of $H_0 + \zeta_{\pm} - \alpha^{-1} \exp(\alpha\zeta_{\pm}) = 0$. In the averaging integral, we can therefore use $\frac{\partial\zeta}{\partial\mathcal{T}} = -\frac{\partial H}{\partial \mathcal{N}}$ to write

$$\begin{aligned} \langle G(\zeta, \mathcal{N}) \rangle &= -\frac{2}{t_p} \int_{\zeta_+}^{\zeta_-} G(\zeta, F(H_0, \zeta)) \left(\frac{\partial H}{\partial \mathcal{N}} \right)^{-1} d\zeta \\ &= \frac{2}{t_p} \int_{\zeta_-}^{\zeta_+} \frac{G(\zeta, F(H_0, \zeta))}{(n+1)^{n/(n+1)} (H_0 + \zeta - \alpha^{-1} \exp(\alpha\zeta))^{n/(n+1)}} d\zeta, \end{aligned} \quad (105)$$

where, by a similar construction

$$t_p = 2 \int_{\zeta_-}^{\zeta_+} \left(\frac{\partial H}{\partial \mathcal{N}} \right)^{-1} d\zeta = 2 \int_{\zeta_-}^{\zeta_+} \frac{d\zeta}{(n+1)^{n/(n+1)} (H_0 + \zeta - \alpha^{-1} \exp(\alpha\zeta))^{n/(n+1)}}. \quad (106)$$

It should be self-evident that the averaging integral therefore depends on H_0 and the parameters of the model only.

Equation (103) therefore becomes a first-order ordinary differential equation in $H_0(T)$. We can show that it has a stable fixed point by showing that the right-hand side changes from positive to negative somewhere as H_0 increases. We do so by computing the asymptotic limits of the terms on the right-hand side of (103) for small and large H_0 ; this also allows us to show that the fixed point occurs because of the retained $O(\delta\epsilon^{-1})$ terms and occurs when H_0 is logarithmically large in ϵ/δ .

We can first show that H_0 must grow when small, by showing that

$$\langle \exp[(2\alpha - 1)\zeta] \rangle - \langle \exp[(\alpha - 1)\zeta] \rangle = \langle \exp((2\alpha - 1)\zeta) - \exp((\alpha - 1)\zeta) \rangle. \quad (107)$$

is then positive. For H_0 small, ζ must also remain small by (104), and we have $H_0 + \zeta - \alpha^{-1} \exp(\alpha\zeta) \sim H_0 - \alpha\zeta^2/2$. Hence $\zeta_{\pm} \sim \pm(2\alpha^{-1}H_0)^{1/2}$ as well as $\exp((2\alpha - 1)\zeta) - \exp((\alpha - 1)\zeta) \sim \alpha\zeta$. Putting $\zeta = (2\alpha^{-1}H_0)^{1/2}z$, the averaging integrals become

$$\int_{\zeta_-}^{\zeta_+} \frac{\exp[(2\alpha - 1)\zeta] - \exp[(\alpha - 1)\zeta]}{(n+1)^{n/(n+1)} (H_0 + \zeta - \alpha^{-1} \exp(\alpha\zeta))^{n/(n+1)}} d\zeta \sim$$

$$2(n+1)^{-n/(n+1)} H_0^{1-n/(n+1)} \int_{-1}^1 \frac{z dz}{(1-z^2)^{n/(n+1)}}, \quad (108)$$

and similarly

$$t_p \sim 2(2\alpha^{-1})^{1/2} (n+1)^{-n/(n+1)} H_0^{1/2-n/(n+1)} \int_{-1}^1 \frac{dz}{(1-z^2)^{n/(n+1)}}, \quad (109)$$

and the right-hand side of (103) is positive, meaning that the fixed point $H_0 = 0$ is unstable and H_0 grows as expected. (Note that it is possible to show that the remaining $O(\delta\epsilon^{-1})$ terms in (103) are in fact the expression in (107) multiplied by the small parameter $\delta\epsilon^{-1}$ at leading order in small H_0 , and therefore do not affect the sign of the right-hand side of (103).)

To show that the resulting growth is bounded, we need to look at the right-hand side of (103) in the limit of large H_0 . Recall that all the averaged terms are of the form $\langle \exp(m\zeta) \rangle$. For $m > 0$, we can define a new variable as $y = H_0^{-1}\alpha^{-1} \exp(\alpha\zeta)$. At leading order in H_0 , the integral is dominated by the contribution from near the upper limit, and

$$\langle \exp(m\zeta) \rangle \sim 2t_p^{-1} m^{-1} \alpha^{m/\alpha} (n+1)^{-n/(n+1)} H_0^{m/\alpha-n/(n+1)} \int_0^1 \frac{dy}{(1-y^{\alpha/m})^{n/(n+1)}}. \quad (110)$$

For $m < 0$, the dominant contribution instead comes from the lower limit. We put $\zeta = -H_0 + y'$, giving at leading order

$$\langle \exp(m\zeta) \rangle \sim 2t_p^{-1} (n+1)^{-n/(n+1)} \exp(-mH_0) \int_0^\infty \frac{\exp(-my') dy'}{y^{m/(n+1)}}. \quad (111)$$

t_p can similarly be computed, but doing so requires contributions from both limits of integration to be accounted for. The result is however immaterial since all the averaged terms on the right-hand side of (103) share the same factor $2t_p^{-1}$. For large H_0 , the right-hand side of (103) is therefore dominated by the first and third terms, with

$$\frac{\partial H_0}{\partial T} \sim t_p^{-1} \left[C_1(\alpha, n) H_0^{(2\alpha-1)/\alpha-n/(n+1)} - \delta\epsilon^{-1} C_2(n) \exp(H_0) \right] \quad (112)$$

where C_1 and C_2 are positive functions of the parameters only.

The exponent on H_0 in the first term is positive since $\alpha > 1$, $n > 1$, and it becomes apparent that the right-hand side changes sign at a value of H_0 that is logarithmically large in $\delta^{-1}\epsilon$, specifically when $H_0^{-(2\alpha-1)/\alpha+n/(n+1)} \exp(H_0) \sim \delta^{-1}\epsilon$; this is the reason why we retained the formally small $\delta\epsilon^{-1}$ terms in (103). Mathematically, the change in sign ensures a stable fixed point and bounded growth. Physically, we see that bounded growth still requires the cavity opening mechanism (which scales as δ) to be present even in the parameter limit of large water supply, where oscillations are rapid and their amplitude changes only slowly.

Still, the solution we have just constructed remains physically entirely unrealistic. The exercise we have gone through was merely designed to show that we do obtain a bounded solution, with a moderately large value of the Hamiltonian H_0 . The reason

why this is physically unrealistic actually resides in the rescaling (93) and the structure of the Hamiltonian system (97): in these solutions, the effective pressure N becomes large and, crucially, oscillates rapidly between negative and positive values, since at leading order, conduit evolution is driven entirely by changes in effective pressure and the melt-driven channel growth term is a higher order correction. These large and negative values of N are not likely to be sustained by a real glacial system, since they should imply flotation of the ice.

References

- K.E. Atkinson, 1989. *An Introduction to Numerical Analysis*, 2nd Edition. J. Wiley & Sons, Ltd., New York.
- G. Evatt and A.C. Fowler, 2007. Cauldron subsidence and subglacial floods. *Ann. Glaciol.*, **45**, 163–168.
- A.C. Fowler, 1999. Breaking the seal at Grimsvötn. *J. Glaciol.*, **45**(151), 506–516.
- J.W. Glen, 1958. The flow law of ice. A discussion of the assumptions made in glacier theory, their experimental foundation and consequences. In *Physics of the Movement of Ice — Symposium at Chamonix 1958*. IASH, pp. 171–183.
- I.J. Hewitt, C. Schoof, and M.A. Werder, 2012. Flotation and free surface flow in a model for subglacial drainage. Part 2. Channel flow. *J. Fluid Mech.*, **702**, 157–188.
- M.H. Holmes, 1995. *Introduction to Perturbation Methods*. Vol. **20** of *Texts in Applied Mathematics*. Springer-Verlag, New York.
- F.S.L. Ng, 1998. Mathematical Modelling of Subglacial Drainage and Erosion. Ph.D. thesis, Oxford University, <http://www.maths.ox.ac.uk/research/theses/>.
- J.F. Nye, 1976. Water flow in glaciers: jökulhlaups, tunnels and veins. *J. Glaciol.*, **17**(76), 181–207.
- C. Schoof, 2010. Ice-sheet acceleration driven by melt supply variability. *Nature*, **468**, 803–806.
- C. Schoof, C.A. Rada, N.J. Wilson, G.E. Flowers, and M. Haseloff, 2014. Oscillatory subglacial drainage in the absence of surface melt. *The Cryosphere*, **8**, 959–976.
- S. Wiggins, 2003. *Introduction to Applied Nonlinear Dynamical Systems*. Text in Applied Mathematics. Springer, New York.

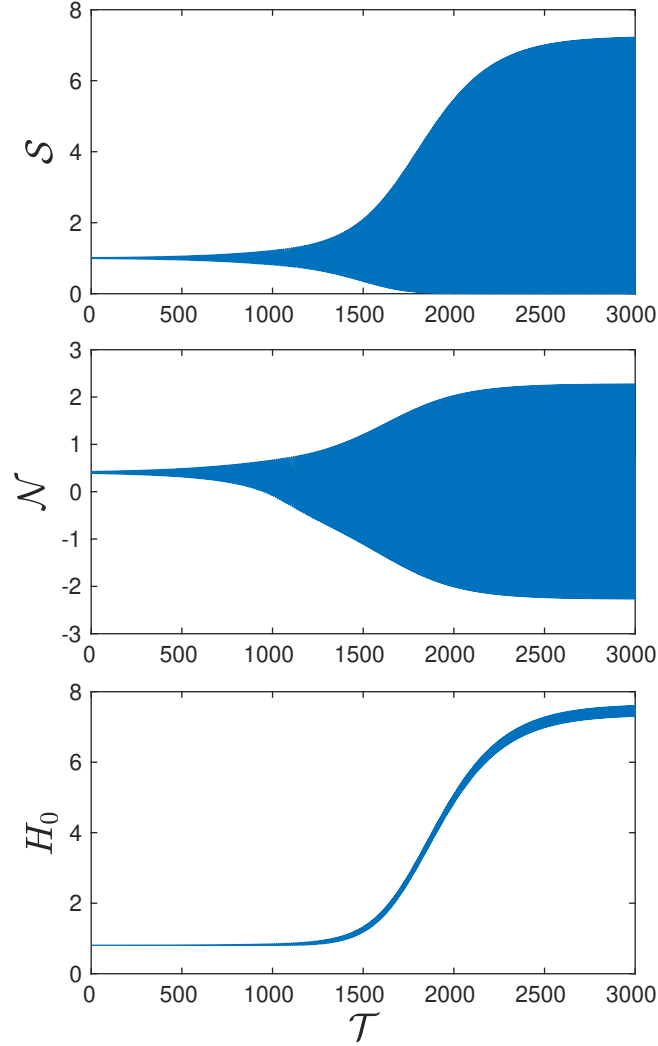


Figure 4: \mathcal{S} , \mathcal{N} and the Hamiltonian H_0 plotted against the inner time variable \mathcal{T} for $\epsilon = 131.5$, $\delta = 1.32 \times 10^{-4}$ and $nu = 6.7 \times 10^{-3}$, $\alpha = 5/4$, $n = 3$ from a solution of the full model (51). The oscillations at the inner time scale are hard to distinguish; the period of the final limit cycle is 5.45. Note that the Hamiltonian H_0 still oscillates in time, but with a far lower amplitude than \mathcal{S} or \mathcal{N} ; this reflects the higher order correction.